

# Proximal algorithms for large-scale statistical modeling and sensor/actuator selection

Armin Zare, Hesameddin Mohammadi, Neil K. Dhingra, Mihailo R. Jovanović, and Tryphon T. Georgiou

## Abstract

Several problems in modeling and control of stochastically-driven dynamical systems can be cast as regularized semi-definite programs. We examine two such representative problems and show that they can be formulated in a similar manner. The first, in statistical modeling, seeks to reconcile observed statistics by suitably and minimally perturbing prior dynamics. The second seeks to optimally select a subset of available sensors and actuators for control purposes. To address modeling and control of large-scale systems we develop a unified algorithmic framework using proximal methods. Our customized algorithms exploit problem structure and allow handling statistical modeling, as well as sensor and actuator selection, for substantially larger scales than what is amenable to current general-purpose solvers. We establish linear convergence of the proximal gradient algorithm, draw contrast between the proposed proximal algorithms and alternating direction method of multipliers, and provide examples that illustrate the merits and effectiveness of our framework.

## Index Terms

Actuator selection, sensor selection, sparsity-promoting estimation and control, method of multipliers, nonsmooth convex optimization, proximal algorithms, regularization for design, semi-definite programming, structured covariances.

## I. INTRODUCTION

Convex optimization has had tremendous impact on many disciplines, including system identification and control design [1]–[7]. The forefront of research points to broadening the range of applications as well as sharpening the effectiveness of algorithms in terms of speed and scalability. The present paper focuses on two representative control problems, statistical control-oriented modeling and sensor/actuator selection, that are cast as convex programs. A range of modern applications require addressing these over increasingly large parameter spaces, placing them outside the reach of standard solvers. A contribution of the paper is to formulate such problems as regularized semi-definite programs (SDPs) and to develop customized optimization algorithms that scale favorably with size.

Financial support from the National Science Foundation under Awards CMMI 1739243, ECCS 1509387 and 1809833, the Air Force Office of Scientific Research under FA9550-16-1-0009, FA9550-17-1-0435, and FA9550-18-1-0422, and ARO under W911NF-17-1-0429 are gratefully acknowledged.

A. Zare, H. Mohammadi, and M. R. Jovanović are with the Ming Hsieh Department of Electrical and Computer Engineering, University of Southern California, Los Angeles, CA 90089. N. K. Dhingra is with Numerica Corporation, Fort Collins, CO 80528. T. T. Georgiou is with the Department of Mechanical and Aerospace Engineering, University of California, Irvine, CA 92697. E-mails: armin.zare@usc.edu, hesamedm@usc.edu, neil.k.dh@gmail.com, mihailo@usc.edu, tryphon@uci.edu.

Modeling is often seen as an inverse problem where a search in parameter space aims to find a parsimonious representation of data. For example, in the control-oriented modeling of fluid flows, it is of interest to improve upon dynamical equations arising from first-principles (e.g., linearized Navier-Stokes equations), in order to accurately replicate observed statistical features that are estimated from data. To this end, a perturbation of the prior model can be seen as a feedback gain that results in dynamical coupling between a suitable subset of parameters [8], [9]. On the flip side, active control of large-scale and distributed systems requires judicious placement of sensors and actuators which again can be viewed as the selection of a suitable feedback or Kalman gain. In either modeling or control, the selection of such gain matrices must be guided by optimality criteria as well as simplicity (low rank or sparse architecture). We cast both types of problems as optimization problems that utilize suitable convex surrogates to handle complexity. The use of such surrogates is necessitated by the fact that searching over all possible architectures is combinatorially prohibitive.

Applications that motivate our study require scalable algorithms that can handle large-scale problems. While the optimization problems that we formulate are SDP representable, e.g., for actuator selection, worst-case complexity of generic solvers scales as the sixth power of the sum of the state dimension and the number of actuators. Thus, solvers that do not exploit the problem structure cannot cope with the demands of such large-scale applications. This necessitates the development of customized algorithms that are pursued herein.

Our presentation is organized as follows. In Section II, we describe the modeling and control problems that we consider, provide an overview of literature and the state-of-the-art, and highlight the technical contribution of the paper. In Section III, we formulate the *minimum energy covariance completion* (control-oriented modeling) and *sensor/actuator selection* (control) problems as nonsmooth SDPs. In Section IV, we present a customized Method of Multipliers (MM) algorithm for covariance completion. An essential ingredient of MM is the proximal gradient method which we also use for sensor/actuator selection. In Section V, we offer two motivating examples for actuator selection and covariance completion and discuss computational experiments. We conclude with a brief summary of the results and future directions in Section VI.

## II. MOTIVATING APPLICATIONS AND CONTRIBUTION

We consider dynamical systems with additive stochastic disturbances. In the first instance, we are concerned with a modeling problem where the statistics are not consistent with a prior model that is available to us. In that case, we seek to modify our model in a parsimonious manner (a sparse and structured perturbation of the state matrix) so as to account for the partially observed statistics. In the second, we are concerned with the control of such stochastic dynamics via a collection of judiciously placed sensors and actuators. Once again, the architecture of the (now) control problem calls for the selection of sparse matrix gains that effect control and estimation. These problems are explained next.

### A. Statistical modeling and covariance completion

It is well-established that the linearized Navier-Stokes (NS) equations driven by stochastic excitation can account for qualitative [10]–[13] and quantitative [9] features of shear fluid flows. The value of such models has been

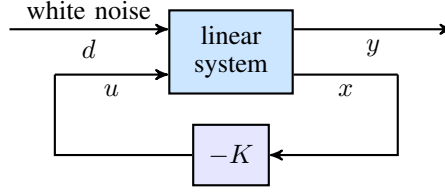


Fig. 1. A feedback connection of an LTI system with a static gain matrix that is designed to account for the sampled steady-state covariance  $X$ .

to provide insights into the underlying physics as well as to guide control design. A significant recent step in this direction was to recognize [9] that *colored-in-time* excitation can account for features of the flow field that *white* noise in earlier literature cannot [14]. Furthermore, it has been pointed out that the effect of colored-in-time excitation is *equivalent* to white-in-time excitation together with a *structural perturbation of the system dynamics* [8], [9]. Such structural perturbations may reveal salient dynamical couplings between variables and, thereby, enhance understanding of basic physics [9, Section 6.1].

These insights and reasoning motivate an optimal state-feedback synthesis problem [15] to identify dynamical couplings that bring consistency between the model and the observed statistics. Model parsimony dictates a penalty on the complexity of structural perturbations and leads to an optimization problem that involves a composite cost function

$$f(X, K) + \gamma g(K), \quad (1)$$

subject to stability of the system in Fig. 1. Here,  $X$  denotes a state covariance matrix and  $K$  is a state-feedback matrix. The function  $f(X, K)$  penalizes variance and control energy while  $g(K)$  is a sparsity-promoting regularizer which penalizes the number of nonzero rows in  $K$ ; sparsity in the rows of  $K$  amounts to a low rank perturbation of the system dynamics. In addition, state statistics may be partially known, in which case a constraint  $X_{ij} = G_{ij}$  for  $(i, j) \in \mathcal{I}$  is added, where the entries of  $G$  represent known entries of  $X$  for indices in  $\mathcal{I}$ .

The resulting *minimum-control-energy covariance completion problem* can be cast as an SDP which, for small-size problems, is readily solvable using standard software. A class of similar problems have been proposed in the context of stochastic control [16]–[19] and of output covariance estimation [20]–[22] which, likewise and for small-size, are readily solvable by standard software.

### B. Sensor and actuator selection

The selection and proper placement of sensors/actuators impacts the performance of closed-loop control systems; making such a choice is a nontrivial task even for systems of modest size. Previous work on actuator/sensor placement either relies on heuristics or on greedy algorithms and convex relaxations.

The benefit of a particular sensors/actuator placement is typically quantified by properties of the resulting controllability/observability gramians and the selection process is guided by indicators of diminishing return in

performance near optimality [23], [24]. However, metrics on the performance of Kalman filters and other control objectives have been shown to lack supermodularity [25], [26], which hampers the effectiveness of greedy approaches in sensor/actuator selection.

The literature on different approaches includes convex formulations for sensor placement in problems with linear measurements [27], maximizing the trace of the Fisher information under constraints when dealing with correlated measurement noise [28], and a variation of optimal experiment design for placing measurement units in power networks [29]. Actuator selection via genetic algorithms has also been explored [30]. Finally, a non-convex formulation of the joint sensor and actuator placement was advanced in [31], [32] and was recently applied to the linearized Ginzburg-Landau equation [33].

Herein, we cast our placement problem as one of optimally selecting a subset of potential sensors or actuators which, in a similar manner as our earlier modeling problem, involves the minimization of a nonsmooth composite function as in (1). More specifically, we utilize the sparsity-promoting framework developed in [34]–[36] to enforce block-sparse structured observer/feedback gains and select sensors/actuators.

The algorithms developed in [36] have been used for sensor selection in target tracking [37] and in periodic sensor scheduling in networks of dynamical systems [38]. However, they were developed for general problems, without exploiting a certain hidden convexity in sensor/actuator selection. Indeed, for the design of row-sparse feedback gains, the authors of [39] introduced a convex SDP reformulation of the problem formulated in [36]. Inspired by [36], the authors of [40] extended the SDP formulation to  $\mathcal{H}_2$  and  $\mathcal{H}_\infty$  sensor/actuator placement problems for discrete time LTI systems. Their approach utilizes standard SDP-solvers with re-weighted  $\ell_1$ -norm regularizers. In the present paper, we integrate several of these ideas. In particular, we borrow group-sparsity regularizers from statistics [41] and develop efficient customized proximal algorithms for the resulting SDPs.

### C. Main contribution

In the present paper, we highlight the structural similarity between statistical modeling and sensor/actuator selection, and develop a unified algorithmic framework for handling large-scale problems. Proximal algorithms are utilized to address the non-differentiability of the sparsity-promoting term  $g(K)$  in the objective function. We exploit the problem structure, implicitly handle the stability constraint on state covariances and controller gains by expressing one in terms of the other, and develop a customized proximal gradient algorithm that scales with the third power of the state-space dimension. We prove linear convergence for the proximal gradient algorithm with fixed step-size and propose an adaptive step-size selection method that can improve convergence. We also discuss initialization techniques and stopping criteria for our algorithms, and provide numerical experiments to demonstrate the effectiveness of our approach relative to existing methods.

### III. PROBLEM FORMULATION

Consider a linear time-invariant (LTI) system with state-space representation

$$\begin{aligned}\dot{x} &= Ax + Bu + d \\ y &= Cx\end{aligned}\tag{2}$$

where  $x(t) \in \mathbb{C}^n$  is the state vector,  $y(t) \in \mathbb{C}^p$  is the output,  $u(t) \in \mathbb{C}^m$  is the control input,  $d(t)$  is a zero-mean white stochastic process with the covariance matrix  $V \succ 0$ ,  $B \in \mathbb{C}^{n \times m}$  is the input matrix with  $m \leq n$ ,  $C \in \mathbb{C}^{p \times n}$  is the output matrix, and the pair  $(A, B)$  is controllable. We consider two specific applications, one that relates system identification and covariance completion, and another that focuses on sensor/actuator selection in a control problem. Both can be cast as the problem to select a stabilizing state-feedback control law,  $u = -Kx$ , that utilizes few input degrees of freedom in the sense that the matrix  $K$  has a large number of zero rows. At the same time, the closed-loop system

$$\dot{x} = (A - BK)x + d,$$

shown in Fig. 1 is consistent with partially available state-correlations and/or is optimal in a quadratic sense.

More specifically, if

$$X := \lim_{t \rightarrow \infty} \mathbf{E}(x(t)x^*(t))$$

denotes the stationary state-covariance of the controlled system, the pertinent quadratic cost is

$$f(X, K) := \text{trace}(QX + K^*RKX) = \lim_{t \rightarrow \infty} \mathbf{E}(x^*(t)Qx(t) + u^*(t)Ru(t)),\tag{3}$$

where  $\mathbf{E}$  is the expectation operator, whereas  $Q = Q^* \succ 0$  and  $R = R^* \succ 0$  specify penalties on the state and control input, respectively. Both stability of the feedback dynamics and consistency with the state covariance  $X$  reduce to an algebraic constraint on  $K$  and  $X$ , namely,

$$(A - BK)X + X(A - BK)^* + V = 0.\tag{4}$$

Finally, the number of non-zero rows of  $K$  can be seen as the number of active degrees of freedom of the input or as the rank of a perturbation  $A - BK$  of  $A$ . The choice of such a  $K$ , with few non-zero rows is sought via minimization of a non-smooth composite objective function

$$J(X, K) := f(X, K) + \gamma g(K),\tag{5}$$

where

$$g(K) := \sum_{i=1}^n w_i \|e_i^* K\|_2\tag{6}$$

is a regularizing term that promotes row-sparsity of  $K$  [41]. Here,  $\gamma > 0$  specifies the importance of sparsity,  $w_i$  are nonzero weights, and  $e_i$  is the  $i$ th unit vector in  $\mathbb{R}^m$ . In what follows, we address the following problem.

*Problem 1:* Minimize  $f(X, K) + \gamma g(K)$ , subject to (4),  $X \succ 0$ , and, possibly, constraints on the values of specified entries of  $X$ ,  $X_{ij} = G_{ij}$  for  $(i, j) \in \mathcal{I}$ , where a set of pairs  $\mathcal{I}$  and the entries  $G_{ij}$  are given.

A useful variant of the constraint on the entries of  $X$ , when, e.g., statistics are estimated on output variables, can be expressed as

$$(CXC^*)_{ij} = G_{ij} \text{ for } (i, j) \in \mathcal{I}, \quad (7)$$

where  $\mathcal{I}$  specifies indices of available covariance data. We explain next how this problem and its variants relate to the two aforementioned topics of covariance completion and sensor/actuator selection.

#### A. Covariance completion and model consistency

In many problems it is often the case that a model is provided for a given process which, however, is inconsistent with new data. In such instances, it is desirable to revise the dynamics by a suitable perturbation to bring compatibility between model and data. The data in our setting consists of statistics in the form of a state covariance  $X$  for a linear model

$$\dot{x} = Ax + d \quad (8)$$

with white noise input  $d$ .

We postulate and deal with a further complication when the data is incomplete. More specifically, we allow  $X$  to be only partially known. Such an assumption is motivated by fluid flow applications that rely on the linearized NS equations [9]. In this area both the numerical and experimental determination of all entries of  $X$  is often prohibitively expensive. Thus, the problem to bring consistency between data and model can be cast in the form of Problem 1, where we seek a completion of the missing entries of  $X$  along with a perturbation  $\Delta := -BK$  of the system dynamics (8), into

$$\dot{x} = (A + \Delta)x + d.$$

The assumed structure of  $\Delta$  is without loss of generality, and the choice of  $B$  may incorporate added insights into the strength and directionality of possible couplings between state variables. Ultimately, the choice of most suitable perturbation will be determined by the optimization criterion. Furthermore, it is also natural to impose a penalty on the average quadratic size of the perturbation signals  $Kx$ , and this brings us exactly into the setting of Problem 1. Once again, the row-sparsity promoting penalty  $g(K)$  impacts directly the rank of the perturbation  $\Delta$  and choice of feedback couplings that need to be introduced to modify the dynamical generator  $A$  [15].

#### B. Actuator selection

As is well-known, the unique optimal control law that minimizes the steady-state variance (3) of system (2) is a static state-feedback  $u = -Kx$ . The optimal gain  $K$  and the corresponding state covariance  $X$  can be obtained by minimizing  $f(X, K)$ , over  $K \in \mathbb{C}^{m \times n}$ , and positive definite  $X = X^* \in \mathbb{C}^{n \times n}$ . The solution can also be obtained by solving an algebraic Riccati equation arising from the KKT conditions of this optimization problem. In general,  $K$

has no particular structure. In fact, generically  $K$  has no zero entries, and therefore all “input channels” (i.e., entries of  $u$ ) are active and non-zero. Since the columns of  $B$  encode the effect of individual “input channels”, representing location of actuators, a subselection that is affected by the row-sparsity promoting regularizer in Problem 1, amounts to actuator selection amongst available options. A dual formulation can be cast to address sensor selection and can be approached in a similar manner; see Appendix A.

### C. Change of variables and SDP representation

The constraint  $X \succ 0$  in Problem 1 allows for a standard change of variables  $Y := KX$  to replace  $K$  in  $f(X, K) = \text{trace}(QX + K^* R K X)$ . This yields a jointly convex function of  $(X, Y)$ ,

$$f(X, Y) = \text{trace}(QX + Y^* R Y X^{-1}). \quad (9)$$

Further, the row-sparsity of  $K$  is equivalent to the row-sparsity of  $Y$  [39]. This observation leads us to the convex reformulation of Problem 1 (incorporating the more general version of constraints (7)) as follows.

*Problem 2:* Minimize  $f(X, Y) + \gamma \sum_i w_i \|e_i^* Y\|_2$  over a Hermitian matrix  $X \in \mathbb{C}^{n \times n}$  and  $Y \in \mathbb{C}^{m \times n}$ , subject to:

$$\begin{aligned} A X + X A^* - B Y - Y^* B^* + V &= 0 \\ (1 - \delta) [(C X C^*) \circ E - G] &= 0 \\ X &\succ 0 \end{aligned}$$

where

$$\delta = \begin{cases} 0, & \text{for covariance completion} \\ 1, & \text{for actuator selection.} \end{cases}$$

The symbol  $\circ$  denotes elementwise matrix multiplication, and  $E$  is the structural identity matrix,

$$E_{ij} = \begin{cases} 1, & \text{if } G_{ij} \text{ is available} \\ 0, & \text{if } G_{ij} \text{ is unavailable.} \end{cases}$$

As explained earlier, the matrices  $A$ ,  $B$ ,  $C$ ,  $G$ , and  $V$  are problem data. From the solution of Problem 2, the optimal feedback gain matrix can be recovered as  $K = Y X^{-1}$ . We note that the optimization of  $f$  can be expressed as an SDP. Specifically, the Schur complement can be used to characterize the epigraph of  $\text{trace}(R Y X^{-1} Y^*)$  via the convex constraints

$$\text{trace}(W) \text{ and } \begin{bmatrix} W & R^{1/2} Y \\ Y^* R^{1/2} & X \end{bmatrix} \succeq 0,$$

where  $W$  is a matrix variable, and the joint convexity of  $\text{trace}(R Y X^{-1} Y^*)$  in  $(X, Y)$  follows [4].

We also note that although the row-sparsity patterns of  $Y$  and  $K$  are equivalent, the weights  $w_i$  are not necessarily the same in the respective expressions in Problems 1 and 2. In practice, the weights are iteratively adapted to promote row-sparsity; see Section IV-G. Problem 2 can be solved efficiently using general-purpose solvers for small number

of variables. To address larger problems, we next exploit the structure and develop optimization algorithms based on the proximal gradient algorithm and the method of multipliers.

#### IV. CUSTOMIZED ALGORITHMS

In this section, we describe the steps through which we solve Problem 2, identify the essential input channels in  $B$ , and subsequently refine the solutions based on the identified sparsity structure. For notational compactness, we write the linear constraints in Problem 2 as

$$\mathcal{A}_1(X) - \mathcal{B}(Y) + V = 0, \quad (1 - \delta)[\mathcal{A}_2(X) - G] = 0$$

where the linear operators  $\mathcal{A}_1: \mathbb{C}^{n \times n} \rightarrow \mathbb{C}^{n \times n}$ ,  $\mathcal{A}_2: \mathbb{C}^{n \times n} \rightarrow \mathbb{C}^{p \times p}$  and  $\mathcal{B}: \mathbb{C}^{m \times n} \rightarrow \mathbb{C}^{n \times n}$  are given by

$$\mathcal{A}_1(X) := AX + XA^*, \quad \mathcal{A}_2(X) := (CXC^*) \circ E, \quad \mathcal{B}(Y) := BY + Y^*B^*.$$

##### A. Elimination of variable $X$

For any  $Y$ , there is a unique  $X$  that solves the equation

$$\mathcal{A}_1(X) - \mathcal{B}(Y) + V = 0$$

if and only if the matrices  $A^*$  and  $-A$  do not have any common eigenvalues [42]. When this condition holds, we can express the variable  $X$  as an affine function of  $Y$ ,

$$X(Y) = \mathcal{A}_1^{-1}(\mathcal{B}(Y) - V), \quad (10)$$

and restate Problem 2 as

$$\begin{aligned} & \underset{Y}{\text{minimize}} && f(Y) + \gamma g(Y) \\ & \text{subject to} && (1 - \delta)[\mathcal{A}_2(X(Y)) - G] = 0 \\ & && X(Y) \succ 0. \end{aligned} \quad (11)$$

The smooth part of the objective function in (11) is given by

$$f(Y) := \text{trace}(QX(Y) + Y^*RYX^{-1}(Y)) \quad (12)$$

and the regularizing term is

$$g(Y) := \sum_{i=1}^n w_i \|e_i^* Y\|_2.$$

Since optimization problem (11) is equivalent to Problem 2 constrained to the affine equality (10), it remains convex.

When the matrix  $A$  is Hurwitz, expression (10) can be cast in terms of the well-known integral representation,

$$X(Y) = \int_0^\infty e^{At} (V - BY - Y^*B^*) e^{A^*t} dt.$$



Even for unstable open-loop systems, the operator  $\mathcal{A}_1$  is invertible if the matrices  $A^*$  and  $-A$  do not have any common eigenvalues. In our customized algorithms, we numerically evaluate the action of  $\mathcal{A}_1^{-1}$  on the current iterate by solving the corresponding Lyapunov equation which requires making the following assumption.

*Assumption 1:* The operator  $\mathcal{A}_1$  is invertible.

Appendix B provides a method to handle cases where this assumption does not hold.

### B. Proximal gradient method for actuator selection

The proximal gradient (PG) method generalizes gradient descent to composite minimization problems in which the objective function is the sum of a differentiable and non-differentiable component [43]. It is most effective when the proximal operator [44] associated with the nondifferentiable component is easy to evaluate; many common regularization functions, such as the  $\ell_1$  penalty, nuclear norm, and hinge loss, satisfy this condition.

The PG method for solving (11) with  $\delta = 1$  is given by

$$Y^{k+1} := \mathbf{prox}_{\beta_k g}(Y^k - \alpha_k \nabla f(Y^k)), \quad (13)$$

where  $k$  is the iteration counter,  $Y^k$  is the  $k$ th iterate,  $\alpha_k > 0$  is the step-size,  $\beta_k := \alpha_k \gamma$ , and  $\mathbf{prox}_{\beta g}(\cdot)$  is the proximal operator associated with the function  $g$

$$\mathbf{prox}_{\beta g}(V) := \underset{Y}{\operatorname{argmin}} \quad g(Y) + \frac{1}{2\beta} \|Y - V\|_F^2. \quad (14)$$

Here,  $\|\cdot\|_F$  is the Frobenius norm and, for row-sparsity regularizer, the proximal operator is determined by the soft-thresholding operator which acts on the rows of the matrix  $V$ ,

$$\mathcal{S}_\beta(e_i^* V) = \begin{cases} (1 - \beta/\|e_i^* V\|_2) e_i^* V, & \|e_i^* V\|_2 > \beta w_i \\ 0, & \|e_i^* V\|_2 \leq \beta w_i. \end{cases}$$

Proximal update (13) results from a local quadratic approximation of  $f$  at iteration  $k$ , i.e.,

$$Y^{k+1} := \underset{Y}{\operatorname{argmin}} \quad f(Y^k) + \langle \nabla f(Y^k), Y - Y^k \rangle + \frac{1}{2\alpha_k} \|Y - Y^k\|_F^2 + \gamma g(Y), \quad (15)$$

followed by a completion of squares that brings the problem into the form of (14). Here,  $\langle \cdot, \cdot \rangle$  denotes the standard matricial inner product  $\langle M_1, M_2 \rangle := \operatorname{trace}(M_1^* M_2)$  and the expression for the gradient of  $f(Y)$  is provided in Appendix C.

1) *Choice of step-size in (13):* At each iteration of the PG method, we determine the step-size  $\alpha_k$  via an adaptive Barzilai-Borwein (BB) initial step-size selection [45], i.e.,

$$\alpha_{k,0} = \begin{cases} \alpha_m & \text{if } \alpha_m/\alpha_s > 1/2 \\ \alpha_s - \alpha_m/2 & \text{otherwise} \end{cases} \quad (16)$$

followed by backtracking to ensure stability of the subsequent iterate

$$X(Y^{k+1}) \succ 0 \quad (17a)$$

and sufficient descent of the objective function

$$f(Y^{k+1}) \leq f(Y^k) + \langle \nabla f(Y^k), Y^{k+1} - Y^k \rangle + \frac{1}{2\alpha_k} \|Y^{k+1} - Y^k\|_F^2. \quad (17b)$$

Similar strategies as (17b) were used in [43, Theorem 3.1]. Here, the “steepest descent” step-size  $\alpha_s$  and the “minimum residual” step-size  $\alpha_m$  are given by [46],

$$\alpha_s = \frac{\langle Y^k - Y^{k-1}, Y^k - Y^{k-1} \rangle}{\langle Y^k - Y^{k-1}, \nabla f(Y^k) - \nabla f(Y^{k-1}) \rangle}, \quad \alpha_m = \frac{\langle Y^k - Y^{k-1}, \nabla f(Y^k) - \nabla f(Y^{k-1}) \rangle}{\langle \nabla f(Y^k) - \nabla f(Y^{k-1}), \nabla f(Y^k) - \nabla f(Y^{k-1}) \rangle}.$$

If  $\alpha_s < 0$  or  $\alpha_m < 0$ , the step-size from the previous iteration is used; see [45, Section 4.1] for additional details.

2) *Stopping criterion:* We employ a combined condition that terminates the algorithm when either the relative residual

$$r_r^{k+1} = \frac{\|r^{k+1}\|}{\max\{\|\nabla f(Y^{k+1})\|, \|\frac{\hat{Y}^{k+1} - Y^{k+1}}{\alpha_k}\|\} + \epsilon_r},$$

or the normalized residual  $r_n^{k+1} = \|r^{k+1}\|/(\|r^1\| + \epsilon_n)$ , are smaller than a desired tolerance. Here,  $\epsilon_r$  and  $\epsilon_n$  are small positive constants, the residual is defined as

$$r^{k+1} := \nabla f(Y^{k+1}) + \frac{\hat{Y}^{k+1} - Y^{k+1}}{\alpha_k},$$

and  $\hat{Y}^{k+1} := Y^k - \alpha_k \nabla f(Y^k)$ . While achieving a small  $r_r$  guarantees a certain degree of accuracy, its denominator nearly vanishes when  $\nabla f(x^*) = 0$ , which happens when  $0 \in \partial g(Y^*)$ . In such cases,  $\|r_n\|$  provides an appropriate stopping criterion; see [45, Section 4.6] for additional details.

---

**Algorithm 1** Customized PG Algorithm

---

**input:**  $A, B, V, Q, R, \gamma > 0$ , positive constants  $\epsilon_r, \epsilon_n$ , tolerance  $\epsilon$ , and backtracking constant  $c \in (0, 1)$ .

**initialize:**  $k = 0, \alpha_{0,0} = 1, r_r^0 = 1, r_n^0 = 1$ , choose  $Y^0 = K_c X_c$  where  $K_c$  and  $X_c$  solve the algebraic Riccati equation that specifies the optimal centralized controller.

**while:**  $r_r^k > \epsilon$  or  $r_n^k > \epsilon$

    compute  $\alpha_k$ : largest feasible step in  $\{c^j \alpha_{k,0}\}_{j=0,1,\dots}$

    such that  $Y^{k+1}$  satisfies (17)

    compute  $r_r^{k+1}$  and  $r_n^{k+1}$

$k = k + 1$

    choose  $\alpha_{k,0}$  based on (16)

**endwhile**

**output:**  $\epsilon$ -optimal solutions,  $Y^{k+1}$  and  $X(Y^{k+1})$ .

---

### C. Linear convergence of the proximal gradient algorithm

In this section, we prove convergence of the proposed PG algorithm. We show that (i) over any sublevel set, the function  $f(Y)$  in (12) and its gradient are strongly convex and Lipschitz continuous, respectively; and (ii) the iterates of the PG algorithm with a small enough step-size remain within a sublevel set. These two facts allow us to establish linear convergence of the PG algorithm. Proofs of all technical statements presented here are provided in Appendix D.

While the gradient  $\nabla f(Y)$  is not Lipschitz continuous over the set

$$\mathcal{D}_s := \{Y \in \mathbb{C}^{m \times n} \mid \mathcal{A}(X(Y)) - \mathcal{B}(Y) = -V, X(Y) \succ 0\},$$

which corresponds to stabilizing feedback gains  $K = YX^{-1}$ , we show that it is Lipschitz continuous over the sublevel sets  $\mathcal{D}(a) := \{Y \in \mathcal{D}_s \mid f(Y) \leq a\}$ . We also show that over any sublevel set  $\mathcal{D}(a)$  the function  $f(Y)$  is strongly convex. The following theorem allows us to establish linear convergence for the PG algorithm.

*Theorem 1:* Over any sublevel set  $\mathcal{D}(a)$ , there exist positive scalars  $\mu$  and  $L$  such that the function  $f$  is  $\mu$ -strongly convex and its gradient  $\nabla f$  is  $L$ -Lipschitz continuous.

Lemma 1 provides an expression for the Lipschitz continuity parameter  $L$  of  $\nabla f$  over sublevel sets  $\mathcal{D}(a)$  in terms of the problem data and the starting point  $Y^0$ .

*Lemma 1:* Over any non-empty sublevel set  $\mathcal{D}(a)$ , the gradient  $\nabla f$  is Lipschitz continuous with parameter

$$L = \frac{2m\lambda_{\max}(R)}{\nu} \left( 1 + \frac{\sigma_{\max}(\mathcal{A}_1^{-1}(\mathcal{B}))a}{\nu\sqrt{\lambda_{\min}(R)\lambda_{\min}(Q)}} \right)^2 \quad (18a)$$

where

$$\nu = \frac{\lambda_{\min}^2(V)}{4a} \left( \frac{\sigma_{\max}(A)}{\sqrt{\lambda_{\min}(Q)}} + \frac{\sigma_{\max}(B)}{\sqrt{\lambda_{\min}(R)}} \right)^{-2}. \quad (18b)$$

In Lemma 2, we show that for small enough step-size  $\alpha_k$  the function value  $f(Y^k)$  in the PG algorithm remains bounded. This allows us to utilize Theorem 1 and establish linear convergence.

*Lemma 2:* Given an initial condition  $Y^0 \in \mathcal{D}_s$  and a scalar  $a > f(Y) + \gamma g(Y)$  for all  $Y \in \mathcal{D}(f(Y^0) + \gamma g(Y^0))$ , the iterates  $\{Y^k\}$  of the PG algorithm with step-size  $\alpha_k \in [0, 1/L]$  satisfy  $Y^k \in \mathcal{D}(a)$ . Here,  $L$  is the Lipschitz continuity parameter of  $\nabla f$  over the sublevel set  $\mathcal{D}(a)$ .

Based on Lemma 2 and Theorem 1, for a step-size  $\alpha_k \in [0, 1/L]$ , the iterates  $\{Y^k\}$  remain in a sublevel set over which  $f(Y)$  is strongly convex and its gradient is Lipschitz continuous. The convergence properties of the PG algorithm follow from standard theory for proximal gradient methods [47, Section 10.6]. In particular, starting from  $Y^0 \in \mathcal{D}_s$ , the PG algorithm converges at a linear rate for a fixed step-size  $\alpha_k \in (0, 1/L]$ . In Appendix E, we establish similar convergence guarantees for the adaptive step-size selection method of Section IV-B1 that does not

require knowledge of the parameter  $L$ .

*Remark 1:* Since the parameter  $L$  in Lemma 2 depends on the initial condition, the convergence rate of the PG algorithm depends both on the step-size and the starting point  $Y^0$ . Furthermore, in Appendix D3, we utilize Lemma 2 to show that any step-size  $\alpha_k \leq 1/L$  satisfies (17).

#### D. Method of multipliers for covariance completion

We handle the additional constraint in the covariance completion problem by employing the Method of Multipliers (MM). MM is the dual ascent algorithm applied to the augmented Lagrangian and it is widely used for solving constrained nonlinear programming problems [48]–[50].

The MM algorithm for constrained optimization problem (11) with  $\delta = 0$  is given by,

$$Y^{k+1} := \underset{Y}{\operatorname{argmin}} \mathcal{L}_{\rho_k}(Y; \Lambda^k) \quad (19a)$$

$$\Lambda^{k+1} := \Lambda^k + \rho_k (\mathcal{A}_2(X(Y^{k+1})) - G), \quad (19b)$$

where  $\mathcal{L}_\rho$  is the associated augmented Lagrangian,

$$\mathcal{L}_\rho(Y; \Lambda) = f(Y) + \gamma g(Y) + \langle \Lambda, \mathcal{A}_2(X(Y)) - G \rangle + \frac{\rho}{2} \|\mathcal{A}_2(X(Y)) - G\|_F^2,$$

$\Lambda \in \mathbb{C}^{p \times p}$  is the Lagrange multiplier and  $\rho$  is a positive scalar. The algorithm terminates when the primal and dual residuals are small enough. The primal residual is given as

$$\Delta_p = \|\mathcal{A}_2(X(Y^{k+1})) - G\|_F, \quad (20a)$$

and the dual residual corresponds to the stopping criterion on subproblem (19a)

$$\Delta_d = \min\{r_r, r_n\}, \quad (20b)$$

where the relative and normal residuals,  $r_r$  and  $r_n$ , are described in Section IV-B.

1) *Solution to the  $Y$ -minimization problem (19a):* For fixed  $\{\rho_k, \Lambda^k\}$ , minimizing the augmented Lagrangian with respect to  $Y$  amounts to finding the minimizer of  $\mathcal{L}_{\rho_k}(Y; \Lambda^k)$  subject to  $X(Y) \succ 0$ . Since  $g(Y)$  is nonsmooth, we cannot use standard gradient descent methods to find the update  $Y^{k+1}$ . However, similar to Section IV-B, a PG method can be used to solve this subproblem iteratively

$$Y^{j+1} = \operatorname{prox}_{\beta_j g}(Y^j - \alpha_j \nabla F(Y^j)), \quad (21)$$

where  $j$  is the inner PG iteration counter,  $\alpha_j > 0$  is the step-size,  $\beta_j := \alpha_j \gamma$ , and  $F(Y)$  denotes the smooth part of the augmented Lagrangian  $\mathcal{L}_{\rho_k}(Y; \Lambda^k)$ ,

$$F(Y) := f(Y) + \langle \Lambda^k, \mathcal{A}_2(X(Y)) - G \rangle + \frac{\rho_k}{2} \|\mathcal{A}_2(X(Y)) - G\|_F^2.$$

The expression for the gradient of  $F(Y)$  is provided in Appendix F. Similar to Section IV-B, we combine BB step-size initialization with backtracking to ensure sufficient descent of  $\mathcal{L}_{\rho_k}(Y; \Lambda^k)$  (cf. (17b)) and positive definiteness of  $X(Y^{j+1})$ .

2) *Lagrange multiplier update and choice of step-size in (19b)*: Customized MM for covariance completion is summarized as Algorithm 2. We follow the procedure outlined in [50, Algorithm 17.4] for the adaptive update of  $\rho_k$ . This procedure allows for inexact solutions of subproblem (19a) and a more refined update of the Lagrange multiplier  $\Lambda$  through the adjustment of convergence tolerances on  $\Delta_p$  and  $\Delta_d$ .

---

**Algorithm 2** Customized MM Algorithm

---

**input:**  $A, B, C, E, G, V, \gamma > 0$ , and tolerances  $\epsilon_p$  and  $\epsilon_d$ .

**initialize:**  $k = 0, \rho_0 = 1, \rho_{\max} = 10^9, \epsilon_0 = 1/\rho_0, \eta_0 = \rho_0^{-0.1}$ , choose  $Y^0 = K_c X_c$  where  $K_c$  and  $X_c$  solve the algebraic Riccati equation that specifies the optimal centralized controller.

**for**  $k = 0, 1, 2, \dots$

solve (19a) using a similar PG algorithm to Algorithm 1  
such that  $\Delta_d \leq \epsilon_k$ .

**if**  $\Delta_p \leq \eta_k$

**if**  $\Delta_p \leq \epsilon_p$  and  $\Delta_d \leq \epsilon_d$

**stop** with approximate solution  $Y^{k+1}$

**else**

$$\begin{aligned}\Lambda^{k+1} &= \Lambda^k + \rho_k (\mathcal{A}_2(X(Y^{k+1})) - G) \\ \rho_{k+1} &= \rho_k, \quad \eta_{k+1} = \max\{\eta_k \rho_{k+1}^{-0.9}, \epsilon_p\} \\ \epsilon_{k+1} &= \max\{\epsilon_k / \rho_{k+1}, \epsilon_d\}\end{aligned}$$

**endif**

**else**

$$\begin{aligned}\Lambda^{k+1} &= \Lambda^k \\ \rho_{k+1} &= \{5\rho_k, \rho_{\max}\}, \quad \eta_{k+1} = \max\{\rho_{k+1}^{-0.1}, \epsilon_p\} \\ \epsilon_{k+1} &= \max\{1/\rho_{k+1}, \epsilon_d\}\end{aligned}$$

**endif**

**endfor**

**output:** optimal solutions,  $Y^{k+1}$  and  $X(Y^{k+1})$ .

---

### E. Computational complexity

Computation of the gradient in both algorithms involves computation of  $X$  from  $Y$  based on (10), a matrix inversion, and solution to the Lyapunov equation. Each of these take  $O(n^3)$  operations as well as an  $O(mn^2)$  matrix-matrix multiplication. The proximal operator for the function  $g$  amounts to computing the 2-norm of all  $m$  rows of a matrix with  $n$  columns, which takes  $O(mn)$  operations. These steps are embedded within an iterative backtracking procedure for selecting the step-size  $\alpha$ . If the step-size selection takes  $q_1$  inner iterations the total computation cost for a single iteration of the PG algorithm is  $O(q_1 n^3)$ . On the other hand, if it takes  $q_2$  iterations for the gradient based method to converge, the total computation cost for a single iteration of our customized MM algorithm is  $O(q_1 q_2 n^3)$ . In contrast, the worst-case complexity of standard SDP solvers is  $O(n^6)$ .

### F. Comparison with other methods

One way of dealing with the lack of differentiability of the objective function in (11) is to split the smooth and nonsmooth parts over separate variables and to add an additional equality constraint to couple these variables. This allows for the minimization of the augmented Lagrangian via the Alternating Direction Method of Multipliers (ADMM) [51].

In contrast to splitting methods, the algorithms considered in this paper use the PG method to solve the nonsmooth problem in terms of the primal variable  $Y$ , thereby avoiding the necessity to update additional auxiliary variables and their corresponding Lagrange multipliers. Moreover, it is important to note that the performance of augmented Lagrangian-based methods is strongly influenced by the choice of  $\rho$ . In contrast to ADMM, there are principled adaptive rules for updating the step-size  $\rho_k$  in MM. Typically, in ADMM, either a constant step-size is used or the step-size is adjusted to keep the norms of primal and dual residuals within a constant factor of one another [51]. Our computational experiments demonstrate that the customized proximal algorithms considered in this paper significantly outperform ADMM.

*Remark 2:* In [52], a customized ADMM algorithm was proposed for solving the optimal sensor and actuator selection problems. In this, the structural Lyapunov constraint on  $X$  and  $Y$  is dualized via the augmented Lagrangian. While this approach does not rely on the invertibility of operator  $\mathcal{A}_1$  (cf. (10)), it involves subproblems that are difficult to solve. Furthermore, as we show in Section V, it performs poorly in practice, especially for large-scale systems. This is because of higher computational complexity ( $O(n^5)$  per iteration) of the ADMM algorithm developed in [52].

### G. Iterative reweighting and polishing

To obtain sparser structures at lower values of  $\gamma$ , we follow [53] and implement a reweighting scheme in which we run the algorithms multiple times for each value of  $\gamma$  and update the weights as  $w_i^{j+1} = 1/(\|e_i^* Y^j\|_2 + \epsilon)$ . Here,  $Y^j$  is the solution in the  $j$ th reweighting step and the small parameter  $\epsilon$  ensures that the weights are well-defined.

After we obtain the solution to problem (11), we conduct a *polishing* step to refine the solution based on the identified sparsity structure. For this, we consider the system

$$\dot{x} = (A - B_{\text{sp}} K) x + d,$$

where the matrix  $B_{\text{sp}} \in \mathbb{C}^{n \times q}$  is obtained by eliminating the columns of  $B$  corresponding to the identified row sparsity structure of  $Y$ , and  $q$  denotes the number of retained input channels. For this system, we solve optimization problem (11) with  $\gamma = 0$ . This step allows us to identify the optimal matrix  $Y \in \mathbb{C}^{q \times n}$  and subsequently the optimal feedback gain  $K \in \mathbb{C}^{q \times n}$  for a system with a lower number of input channels.

## V. NUMERICAL EXPERIMENTS

We provide two examples to demonstrate the utility of the optimization framework for optimal sensor/actuator selection and covariance completion problems and highlight the computational efficiency of our customized algo-

rithms.

#### A. Actuator selection

The Swift-Hohenberg equation is a partial differential equation that has been widely used as a model for studying pattern formations in hydrodynamics and nonlinear optics [54]. Herein, we consider the linearized Swift-Hohenberg equation around its time independent spatially periodic solution [55]

$$\partial_t \psi(t, \xi) = -(\partial_x^2 + 1)^2 \psi(t, \xi) - c \psi(t, \xi) + f \psi(t, \xi) + u(t, \xi) + d(t, \xi),$$

with periodic boundary conditions on a spatial domain  $\xi \in [0, 2\pi]$ . Here, the state  $\psi(t, \xi)$  denotes the fluctuation field,  $u(t, \xi)$  is a spatio-temporal control input,  $d(t, \xi)$  is a zero-mean additive white noise,  $c$  is a constant bifurcation parameter, and we assume that  $f(\xi) := \alpha \cos(\omega\xi)$  with  $\alpha \in \mathbb{R}$ . Finite dimensional approximation using the spectral collocation method yields the following state-space representation

$$\dot{\psi} = A\psi + u + d. \quad (22)$$

For  $c = -0.2$ ,  $\alpha = 2$ , and  $\omega = 1.25$ , the linearized dynamical generator has two unstable modes. We set  $Q = I$  and  $R = 10I$  and solve the actuator selection problem (problem (11) with  $\delta = 1$ ) for 32, 64, 128 and 256 discretization points and for various values of the regularization parameter  $\gamma$ . For  $\gamma = 10$ , Table I compares the proposed PG algorithm against SDPT3 [56] and the ADMM algorithm of [52]. Both PG and ADMM were initialized with  $Y^0 = K_c X_c$ , where  $K_c$  and  $X_c$  solve the algebraic Riccati equation which specifies the optimal centralized controller. This choice guarantees that  $X(Y^0) \succ 0$ . All algorithms were implemented in Matlab and executed on a 2.9 GHz Intel Core i5 processor with 16 GB RAM. The parser CVX [57] was used to call the solver SDPT3. The algorithms terminate when an iterate achieves a certain distance from optimality, i.e.,  $\|X^k - X^*\|_F / \|X^*\|_F < \epsilon$  and  $\|Y^k - Y^*\|_F / \|Y^*\|_F < \epsilon$ . The choice of  $\epsilon = 10^{-3}$  guarantees that the value of the objective function is within 0.01% of optimality. For  $n = 256$ , CVX failed to converge. In this case, iterations are run until the relative or normalized residuals defined in Section IV-B2 become smaller than  $10^{-2}$ .

For  $n = 128$  and 256, ADMM did not converge to desired accuracy in reasonable time. Typically, the ADMM algorithm of [52] computes low-accuracy solutions quickly but obtaining higher accuracy requires precise solutions to subproblems. The iterative reweighting scheme of Section IV-G can be used to improve the sparsity patterns that are identified by such low-accuracy solutions. Nonetheless, Fig. 2 shows that even for larger tolerances, PG is faster than ADMM.

As  $\gamma$  increases in Problem 2, more and more actuators are dropped and the performance degrades monotonically. For  $n = 64$ , Fig. 3(a) shows the number of retained actuators as a function of  $\gamma$  and Fig. 3(b) shows the percentage of performance degradation as a function of the number of retained actuators. Figure 3(b) also illustrates that for various numbers of retained actuators, the solution to convex optimization problem (11) with  $\delta = 1$  consistently

TABLE I  
COMPARISON OF DIFFERENT ALGORITHMS (IN SECONDS) FOR DIFFERENT NUMBER OF DISCRETIZATION POINTS  $n$  AND  $\gamma = 10$ .

| $n$ | CVX    | PG     | ADMM   |
|-----|--------|--------|--------|
| 32  | 12.39  | 6.2    | 362.4  |
| 64  | 268.11 | 51.9   | 4182.6 |
| 128 | 8873.3 | 875.8  | —      |
| 256 | —      | 3872.1 | —      |

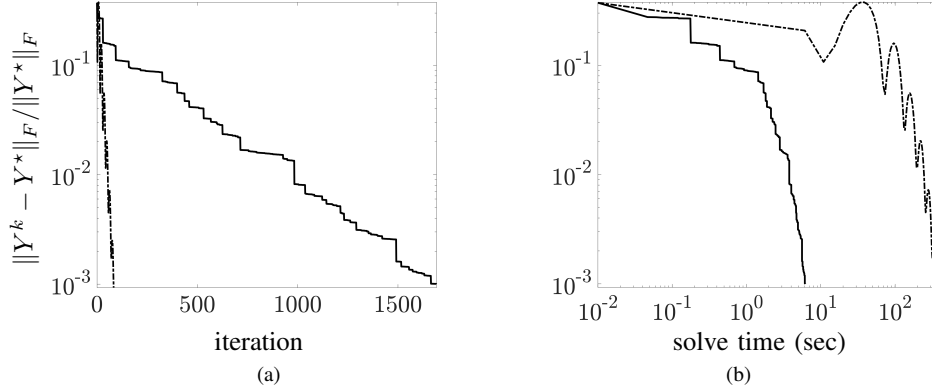


Fig. 2. Convergence curves showing performance of PG (—) and ADMM (— · —) vs. (a) the number of outer iterations; and (b) solve times for the Swift-Hohenberg problem with  $n = 32$  discretization points and  $\gamma = 10$ . Here,  $Y^*$  is the optimal value for  $Y$ .

yields performance degradation that is no larger than the performance degradation of a greedy algorithm (that drops actuators based on their contribution to the  $\mathcal{H}_2$  performance index). For example, the greedy algorithm leads to 24.6% performance degradation when 30 actuators are retained whereas our approach yields 20% performance degradation for the same number of actuators. This greedy heuristic is summarized in Algorithm 3, where  $S$  is the set of actuators and  $f(S)$  denotes the performance index resulting from the actuators within the set  $S$ . When the individual subproblems for choosing fixed numbers of actuators can be executed rapidly, greedy algorithms provide a viable alternative. There has also been recent effort to prove the optimality of such algorithms for certain classes of problems [58]. However, in our example, the greedy algorithm does not always provide the optimal set of actuators with respect to the  $\mathcal{H}_2$  performance index. Relative to the convex formulation, similar greedy techniques yield suboptimal sensor selection for a flexible aircraft wing [7, Section 5.2].

The absence of the sparsity promoting regularizer in Problem 2 leads to the optimal centralized controller which can be obtained from the solution to the algebraic Riccati equation. For  $n = 64$ , Figs. 4(a) and 4(b) show this centralized feedback gain and the two norms of its rows, respectively. For  $\gamma = 0.4$ , 21 of 64 possible actuators are retained and the corresponding optimal feedback gain matrix and row norms are shown in Figs. 4(c) and 4(d). Figure 4(d) also shows that a truncation of the centralized feedback gain matrix based on its row-norms (marked



---

**Algorithm 3** A greedy heuristic for actuator selection
 

---

**input:**  $A, B, V, Q, R$ .

**initialize:**  $\Pi \leftarrow \{1, \dots, m\}$ .

**while:**  $|\Pi| > 0$  and  $f(S) < \infty$ 

$$e^* = \underset{e \in \Pi}{\operatorname{argmin}} f(\Pi) - f(\Pi \setminus \{e\})$$

$$\Pi \leftarrow \Pi \setminus \{e\}$$

**endwhile**
**output:** the set of actuators represented by the set  $\Pi$ .
 

---

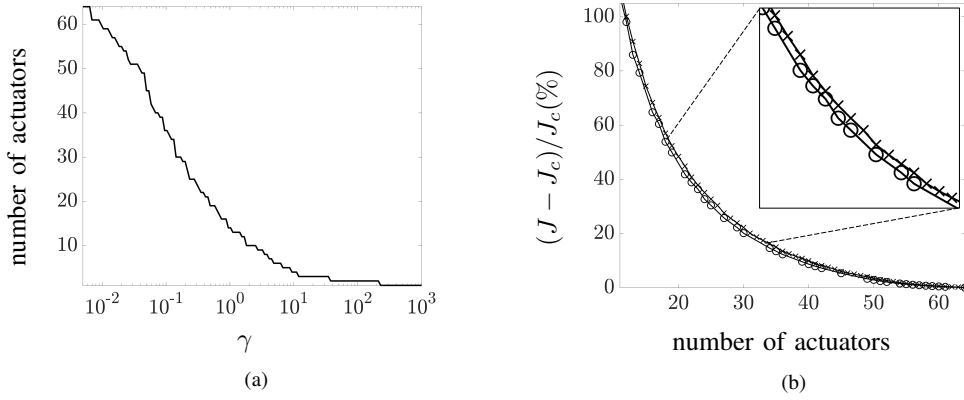


Fig. 3. (a) Number of actuators as a function of the sparsity-promoting parameter  $\gamma$ ; and (b) performance comparison of the optimal feedback controller resulting from the regularized actuator selection problem ( $\circ$ ) and from the greedy algorithm ( $\times$ ) for the Swift-Hohenberg problem with  $n = 64$ .

by blue  $*$  symbols) yields a different subset of actuators than the solution to Problem 2.

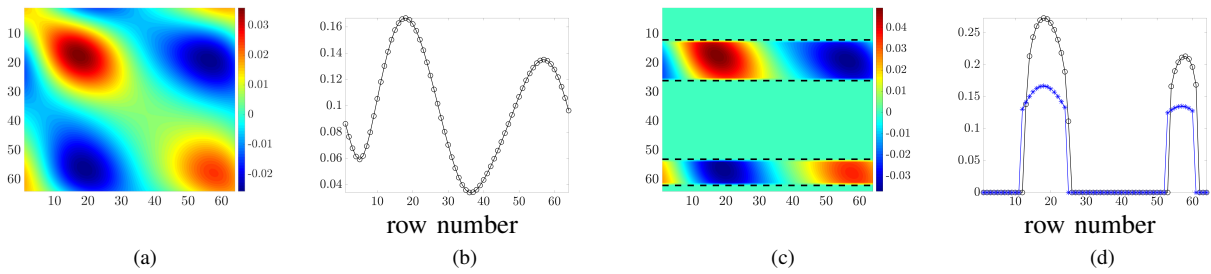


Fig. 4. (a) Optimal centralized feedback gain matrix and (b) its row-norms corresponding to the Swift-Hohenberg dynamics (22) with  $n = 64$ . (c) The optimal feedback gain matrix and (d) its row-norms ( $\circ$ ) resulting from solving Problem 2 with  $\delta = 1$  and  $\gamma = 0.4$  in which the rows between the dashed lines have been retained and polished via optimization. The result of truncating the centralized feedback gain matrix based on its row-norms is shown using blue  $*$  symbols.

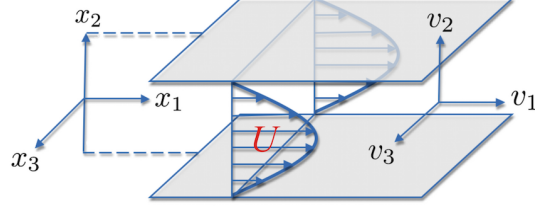


Fig. 5. Geometry of a three-dimensional pressure-driven channel flow.

### B. Covariance completion

We provide an example to demonstrate the utility of our modeling and optimization framework for the purpose of completing partially available second-order statistics of a three-dimensional channel flow. In an incompressible channel-flow, the dynamics of infinitesimal fluctuations around the parabolic mean velocity profile,  $\bar{\mathbf{u}} = [U(x_2) \ 0 \ 0]^T$  with  $U(x_2) = 1 - x_2^2$ , are governed by the Navier-Stokes equations linearized around  $\bar{\mathbf{u}}$ . The streamwise, wall-normal, and spanwise coordinates are represented by  $x_1$ ,  $x_2$ , and  $x_3$ , respectively; see Fig. 5 for geometry. Finite dimensional approximation via application of the Fourier transform in horizontal dimensions ( $x_1$  and  $x_3$ ) and spatial discretization of the wall-normal dimension ( $x_2$ ) using  $N$  collocation points, yields the following state-space representation

$$\begin{aligned} \dot{\boldsymbol{\psi}}(\mathbf{k}, t) &= \mathbf{A}(\mathbf{k}) \boldsymbol{\psi}(\mathbf{k}, t) + \boldsymbol{\xi}(\mathbf{k}, t), \\ \mathbf{v}(\mathbf{k}, t) &= \mathbf{C}(\mathbf{k}) \boldsymbol{\psi}(\mathbf{k}, t). \end{aligned} \quad (23a)$$

Here,  $\boldsymbol{\psi} = [v_2^T \ \eta^T]^T \in \mathbb{C}^{2N}$  is the state of the linearized model,  $v_2$  and  $\eta = \partial_{x_3} v_1 - \partial_{x_1} v_3$  are the normal velocity and vorticity, the output  $\mathbf{v} = [v_1^T \ v_2^T \ v_3^T]^T \in \mathbb{C}^{3N}$  denotes the fluctuating velocity vector,  $\boldsymbol{\xi}$  is a stochastic forcing disturbance,  $\mathbf{k} = [k_1 \ k_3]^T$  denotes the vector of horizontal wavenumbers, and the input matrix is the identity  $I_{2N \times 2N}$ . The dynamical matrix  $\mathbf{A} \in \mathbb{C}^{2N \times 2N}$  and output matrix  $\mathbf{C} \in \mathbb{C}^{3N \times 2N}$  are described in [12].

We assume that the stochastic disturbance  $\boldsymbol{\xi}$  is generated by a low-pass filter with state-space representation

$$\dot{\boldsymbol{\xi}}(\mathbf{k}, t) = -\boldsymbol{\xi}(\mathbf{k}, t) + \mathbf{w}(t), \quad (23b)$$

where  $w$  denotes a zero mean unit variance white process. The steady-state covariance of system (23) can be obtained as a solution to the Lyapunov equation

$$\begin{aligned} \tilde{\mathbf{A}} \boldsymbol{\Sigma} + \boldsymbol{\Sigma} \tilde{\mathbf{A}}^* + \tilde{\mathbf{B}} \tilde{\mathbf{B}}^* &= 0 \\ \tilde{\mathbf{A}} &= \begin{bmatrix} \mathbf{A} & \mathbf{I} \\ \mathbf{O} & -\mathbf{I} \end{bmatrix}, \quad \tilde{\mathbf{B}} = \begin{bmatrix} 0 \\ \mathbf{I} \end{bmatrix}, \quad \boldsymbol{\Sigma} = \begin{bmatrix} \boldsymbol{\Sigma}_{11} & \boldsymbol{\Sigma}_{12} \\ \boldsymbol{\Sigma}_{12}^* & \boldsymbol{\Sigma}_{22} \end{bmatrix}. \end{aligned}$$

The matrix  $\boldsymbol{\Sigma}_{11}$  denotes the steady-state covariance of system (23a)

$$\boldsymbol{\Sigma}_{11} := \lim_{t \rightarrow \infty} \mathbf{E}(\boldsymbol{\psi}(t) \boldsymbol{\psi}^*(t)),$$

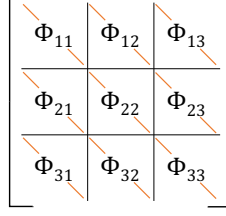


Fig. 6. Structure of the output covariance matrix  $\Phi$ . Available one-point velocity correlations in the normal direction represent diagonal entries of the blocks in the velocity covariance matrix  $\Phi$ .

which, at any wavenumber pair  $\mathbf{k}$ , is related to the steady-state covariance matrix of the output  $\mathbf{v}$  via

$$\Phi(\mathbf{k}) = C(\mathbf{k}) \Sigma_{11}(\mathbf{k}) C^*(\mathbf{k}).$$

Figure 6 shows the structure of the output covariance matrix  $\Phi$ .

In this example, we set the covariance of white noise disturbances to the identity ( $V = I$ ) and assume that the one-point velocity correlations, or diagonal entries of the subcovariance matrices in Fig. 6 are available. In order to account for these available statistics, we solve Problem 2 with  $R = I$  and  $Q = 0$  for a state covariance  $X$  that agrees with the available statistics.

Computational experiments are conducted for a flow with Reynolds number  $10^3$ , the wavenumber pair  $(k_1, k_3) = (0, 1)$ , for various number of collocation points  $N$  in the wall-normal direction (state dimension  $n = 2N$ ), and for various values of the regularization parameter  $\gamma$ . As stated in Algorithm 2, we initialize algorithms using the optimal centralized controller,  $Y^0 := K_c X_c$ . This choice guarantees that  $X(Y^0) \succ 0$ . Our MM algorithm is compared against SDPT3 and ADMM where CVX is used to call SDPT3. When CVX can compute the optimal solution of Problem 2, for each method, iterations are run until the solutions come to within 5% of the CVX solution. For larger problems, iterations are run until the primal and dual residuals satisfy certain tolerances;  $\epsilon_p$ ,  $\epsilon_d = 10^{-2}$ . For  $\gamma = 10$ , Table II compares various methods based on run times (sec). For  $N = 51$  and 101, CVX failed to converge and ADMM did not converge in a reasonable time. Clearly, MM outperforms ADMM. This can also be deduced from Fig. 7, which shows convergence curves for 14 steps of MM and 500 steps of ADMM for  $N = 31$  and  $\gamma = 10$ . For this example, Fig. 8 shows the convergence of MM based on the normalized primal residual  $\Delta_p / \|G\|_F$  and the dual residual  $\Delta_d$  defined in (20).

We now focus on  $N = 51$  collocation points and solve Problem 2 for various values of  $\gamma$ . Since the input matrix  $B$  is assumed to be the identity, the number of inputs  $u$  in this case is  $m = 102$ . Figure 9 shows the  $\gamma$ -dependence of the number of retained input channels that result from solving Problem 2. As  $\gamma$  increases, more and more input channels are dropped. One of the features of our framework is the covariance completion problem

TABLE II  
COMPARISON OF DIFFERENT ALGORITHMS (IN SECONDS) FOR DIFFERENT NUMBER OF DISCRETIZATION POINTS  $N$  AND  $\gamma = 10$ .

| N   | CVX   | MM     | ADMM   |
|-----|-------|--------|--------|
| 11  | 9.3   | 0.19   | 3.10   |
| 21  | 97.67 | 5.6    | 113.4  |
| 31  | 900   | 7.19   | 574.44 |
| 51  | -     | 34.76  | —      |
| 101 | -     | 146.51 | —      |

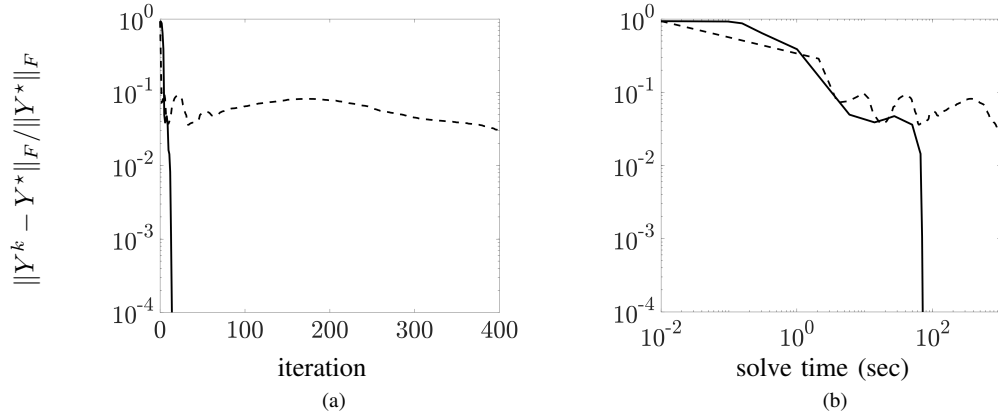


Fig. 7. Convergence curves showing performance of MM (—) and ADMM (---) versus (a) the number of outer iterations; and (b) solve times for  $N = 31$  collocation points in the normal direction  $x_2$  and  $\gamma = 10$ . Here,  $Y^*$  is the optimal value for  $Y$ .

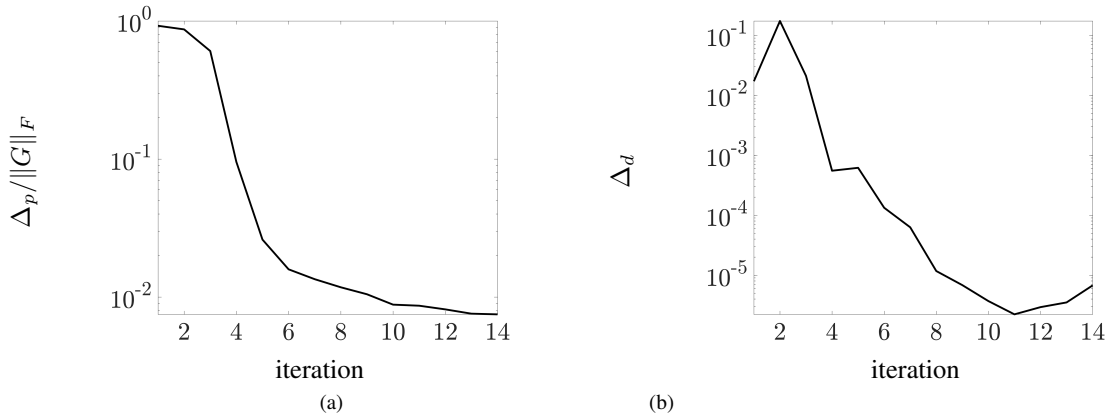


Fig. 8. Performance of MM for the fluids example with  $N = 31$  collocation points in the normal direction  $x_2$  and  $\gamma = 10$ . (a) normalized primal residual; and (b) dual residual based on (20).

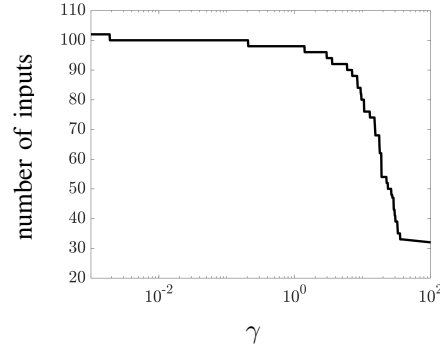


Fig. 9. The  $\gamma$ -dependence of the number of input channels that are retained after solving optimization problem (11) for the channel flow problem with  $m = 101$  inputs.

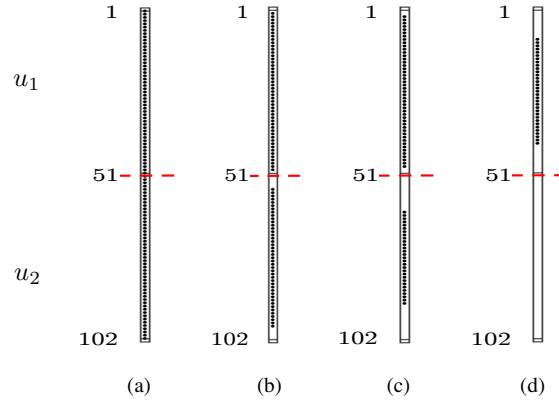


Fig. 10. The input channels in  $u$  that remain effective when problem (11) is solved for the channel flow problem with  $m = 101$  inputs and (a)  $\gamma = 0$ , (b)  $\gamma = 0.1$ , (c)  $\gamma = 10$ , and (d)  $\gamma = 100$ .

not only determines the number of input channels necessary to satisfy the structural constraints on matrices  $X$  and  $Y$ , but it also identifies their directionality. In other words, the row-sparsity of the solution  $Y^*$  determines which inputs in  $u$  play a role in matching the available statistics in a way that is consistent with the linearized dynamics. Figure 10 shows the input channels that are retained via optimization for different values of  $\gamma$ . This figure illustrates the dominant role of input channels that enter the dynamics of normal velocity  $v_2$  and away from the boundaries of the channel. In favor of brevity, we do not expand on the physical interpretations of such findings.

Figures 11(b,d) show the streamwise, and the streamwise/normal two-point correlation matrices resulting from solving (11) with  $\gamma = 100$ . These are, respectively, the  $(1,1)$  and  $(1,2)$  subcovariance matrices in the output covariance matrix  $\Phi$  illustrated in Fig. 6. Even though only one-point velocity correlations along the main diagonal of these matrices were used as problem data in Problem 2, we observe reasonable recovery of off-diagonal terms of the full two-point velocity correlation matrices and 82% of the original output covariance matrix  $\Phi$  is recovered. This quality of completion is consistently observed for various values of  $\gamma$  that do not result in the elimination of the

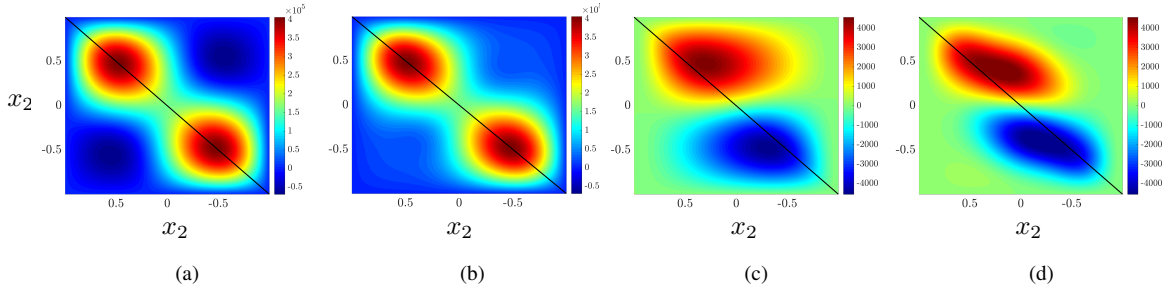


Fig. 11. True covariance matrices of the output velocity field (a, c), and covariance matrices resulting from solving problem (11) (b, d) with  $\gamma = 100$  and  $N = 51$ . (a, b) Streamwise  $\Phi_{11}$ , and (c, d) streamwise/normal  $\Phi_{12}$  two-point correlation matrices at  $\mathbf{k} = (0, 1)$ . One-point correlation profiles that are used as problem data are marked along the main diagonals.

critical input channels in the direction of normal velocity, and is an artifact of including the Lyapunov-like constraint in our formulation. This allows us to retain the relevance of the system dynamics and, thereby, the physics of the problem while matching the partially available statistical signatures of the underlying dynamical system. Additional details regarding the stochastic modeling of turbulent flow statistics and the importance of predicting two-point velocity correlations can be found in [9].

## VI. CONCLUDING REMARKS

We have examined two problems that arise in modeling and control of stochastically driven dynamical systems. The first addresses the modeling of second-order statistics by a parsimonious perturbation of system dynamics, while the second deals with the optimal selection of sensors/actuators for estimation/control purposes. We have shown that both problems can be viewed as the selection of suitable feedback gains, guided by similar optimality metrics and subject to closed-loop stability constraints. We cast both problems as optimization problems and use convex surrogates from group-sparsity paradigm to address combinatorial complexity of searching over all possible architectures. While these are SDP representable, the applications that drive our research give rise to the need for scalable algorithms that can handle large problem sizes. We develop a unified algorithmic framework to address both problems using proximal methods. Our algorithms allow handling statistical modeling, as well as sensor and actuator selection, for substantially larger scales than what is amenable to current general-purpose solvers.

In this work, row sparsity is promoted by penalizing a weighted sum of row norms of the feedback gain matrix. While we note that iterative reweighting [53] can improve the row-sparsity patterns determined by this convex approximation of cardinality, the efficacy of more refined approximations, namely low-rank inducing norms [59], [60], for which proximal operators can be efficiently computed, is a subject of future research. Moreover, we will investigate solving these problems via primal-dual algorithms based on the proximal augmented Lagrangian [61], [62], and proximal Newton-type methods [63], [64].

## ACKNOWLEDGMENTS

We would like to thank Meisam Razaviyayn for useful discussions.

## APPENDIX

## A. Sensor selection

Consider the LTI system

$$\begin{aligned}\dot{x} &= A_s x + d \\ y &= C x + \eta\end{aligned}$$

where  $y$  denotes measurement data which is corrupted by additive white noise  $\eta$ . If  $(A, C)$  is observable, the observer

$$\dot{\hat{x}} = A_s \hat{x} + L C (x - \hat{x}) + L \eta$$

provides an estimate  $\hat{x}$  of the state  $x$ , where  $L$  is the observer gain. When  $A_s - LC$  is Hurwitz, the zero-mean estimate of  $x$  is given by  $\hat{x}$ . The Kalman gain minimizes the steady-state variance of  $x - \hat{x}$ , it is obtained by solving a Riccati equation, and, in general, has no particular structure and uses all available measurements.

Designing a Kalman filter which uses a subset of the available sensors is equivalent to designing a column-sparse Kalman gain matrix  $L$ . Based on this, the optimal sensor selection problem can be addressed by solving the following regularized optimization problem

$$\begin{aligned}& \underset{L, X}{\text{minimize}} \quad \text{trace}(X V_d + L V_\eta L^* X) + \gamma \sum_{i=1}^n w_i \|L e_i\|_2 \\& \text{subject to} \quad (A_s - L C)^* X + X(A_s - L C) + C^* C = 0 \\& \quad X \succ 0\end{aligned}\tag{24}$$

where  $\gamma$ ,  $w_i$ ,  $e_i$  are as described in Problem 1,  $V_d \succ 0$  is the covariance of  $d$ , and  $V_\eta \succ 0$  is the covariance of  $\eta$ . By setting the problem data in Problem 1 to

$$A = A_s^*, \quad B = C^*, \quad Q = V_d, \quad V = C^* C, \quad R = V_\eta,$$

the solution to problem (24) can be obtained from the solution to the actuator selection problem as  $X$  and  $L = K^*$ .

B. Non-invertibility of  $\mathcal{A}_1$ 

In cases where the matrix  $X$  cannot be expressed via (10), since  $(A, B)$  is a controllable pair we can center the design variable around a stabilizing controller  $K_0$ , i.e., by letting  $K := K_0 + K_1$ , where  $K_0$  is held fixed and  $K_1$  is the design variable. Based on this, the change of variables introduced in Section III-C yields  $Y = K_0 X + K_1 X := K_0 X + Y_1$  and  $X(Y_1) = \hat{\mathcal{A}}_1^{-1}(B(Y_1) - V)$  with

$$\hat{\mathcal{A}}_1(X) := (A - B K_0) X + X(A - B K_0)^*.\tag{25}$$

The resulting optimization problem,

$$\begin{aligned} & \underset{Y_1}{\text{minimize}} && f(Y_1) + \gamma g(Y_1 + K_0 X(Y_1)) \\ & \text{subject to} && (1 - \delta)[\mathcal{A}_2(X(Y_1)) - G] = 0 \\ & && X(Y_1) \succ 0 \end{aligned}$$

involves a nonsmooth term  $g$  which is not separable in  $Y_1$ , and the smooth term is given by

$$f(Y_1) := \text{trace}(Q X(Y_1)) + \text{trace}((Y_1 + K_0 X(Y_1))^* R (Y_1 + K_0 X(Y_1)) X^{-1}).$$

Although convex,  $g(Y_1 + K_0 X(Y_1))$  does not have an easily computable proximal operator, making it difficult to apply algorithms that are based on proximal methods.

In this case, one may begin with an input matrix  $B^0$  such that the pair  $(A, B^0)$  is stabilizable and the nonzero columns of  $B^0$  correspond to a subset of input channels  $\mathcal{I}$  that *always* remain active. It would thus be desired to search over input channels from the complement of  $\mathcal{I}$  via the following optimization problem

$$\begin{aligned} & \underset{Y_1}{\text{minimize}} && f(Y_1) + \gamma \hat{g}(Y_1) \\ & \text{subject to} && (1 - \delta)[\mathcal{A}_2(X(Y_1)) - G] = 0 \\ & && X(Y_1) \succ 0. \end{aligned}$$

The operator  $\hat{\mathcal{A}}_1$  in (25) would now be defined using  $B^0$  and the fixed feedback gain matrix  $K_0$  that abides the row-sparsity structure corresponding to  $\mathcal{I}$ . The regularization term  $\hat{g}(Y_1) := \sum_{i \notin \mathcal{I}} w_i \|e_i^* Y_1\|_2$  is used to impose row-sparsity on the *remaining* input channels  $i \notin \mathcal{I}$  and has an easily computable proximal operator, thus facilitating the use of proximal methods. It is noteworthy that this approach may also be employed to obtain an operator  $\hat{\mathcal{A}}_1$  which is better conditioned than  $\mathcal{A}_1$ .

The alternative approach would be to avoid this problem altogether by not expressing  $X$  as a function of  $Y$  and directly dualizing the Lyapunov constraint on  $X$  and  $Y$  via augmented Lagrangian based methods, e.g., ADMM [52]. However, as we show in Section V, such approaches do not lead to algorithms that are computationally efficient for large problems.

### C. Gradient of $f(Y)$ in (13)

To find  $\nabla f(Y)$  in (13), we expand  $f(Y + \epsilon \tilde{Y})$  around  $Y$  for the variation  $\epsilon \tilde{Y}$ , and collect terms of  $O(\epsilon)$ . We also account for the variation of  $X$  as a result of the variation of  $Y$  from

$$(X + \epsilon \tilde{X})^{-1} = X^{-1} - \epsilon X^{-1} \tilde{X} X^{-1} + O(\epsilon^2),$$

and the linear dependence of  $\tilde{X}$  on  $\tilde{Y}$ , i.e.,

$$\tilde{X} = \mathcal{A}^{-1}(\mathcal{B}(\tilde{Y})).$$



Based on this, at the  $k$ th iteration, the gradient of  $f$  with respect to  $Y$  is given by,

$$\nabla f(Y^k) = 2RY^kX^{-1} - 2B^*(W_2 - W_1),$$

where  $W_1$  and  $W_2$  are solutions to the following Lyapunov equations

$$\begin{aligned} A^*W_1 + W_1A + X^{-1}Y^{k*}RY^kX^{-1} &= 0 \\ A^*W_2 + W_2A + Q &= 0 \end{aligned}$$

and  $X^{-1}$  denotes the inverse of  $X(Y^k)$ .

#### D. Proofs of Section IV-C

1) *Proof of Theorem 1:* We first utilize previously established properties of the set of stabilizing feedback gains to prove that the sublevel sets  $\mathcal{D}(a)$  of the function  $f(Y)$  are compact. We then prove that for any convex compact set  $\mathcal{C} \subset \mathcal{D}_s$  there exist a strong convexity module  $\mu > 0$  and a smoothness parameter  $L > 0$  for  $f(Y)$  over  $\mathcal{C}$ .

Consider the function  $Y(K) := KX(K)$  where  $K$  belongs to the set of stabilizing feedback gains  $\mathcal{K}_s$  and  $X(K) \succ 0$  is the unique solution to the algebraic Lyapunov equation (4). The function  $X(K)$  is continuous and the sublevel sets of the function  $f(Y(K))$

$$\mathcal{K}(a) := \{K \in \mathcal{K}_s \mid f(Y(K)) \leq a\}$$

are compact [65]. Since the sublevel set  $\mathcal{D}(a)$  is the image of the compact set  $\mathcal{K}(a)$  under the continuous map  $Y(K)$ , it follows that  $\mathcal{D}(a)$  is also compact.

The next lemma provides an expression for the second-order approximation of the function  $f(Y)$ .

*Lemma 3:* The Hessian of the function  $f(Y)$  satisfies

$$\left\langle \tilde{Y}, \nabla^2 f(Y; \tilde{Y}) \right\rangle = 2 \|R^{\frac{1}{2}}(\tilde{Y} - YX^{-1}\mathcal{M}(\tilde{Y}))X^{-\frac{1}{2}}\|_F^2,$$

where  $X = \mathcal{A}_1^{-1}(\mathcal{B}(Y) - V)$  and  $\mathcal{M}(\tilde{Y}) := \mathcal{A}_1^{-1}(\mathcal{B}(\tilde{Y}))$ .

*Proof:* For any  $Y \in \mathcal{D}_s$  and  $X = \mathcal{A}_1^{-1}(\mathcal{B}(Y) - V)$ , the function  $f(X, Y)$  in Problem 2 reduces to  $f(Y)$ . The second-order approximation of  $f(Y)$  is determined by

$$f(Y + \tilde{Y}) \approx f(Y) + \left\langle \nabla f(Y), \tilde{Y} \right\rangle + \frac{1}{2} \left\langle \tilde{Y}, \nabla^2 f(Y; \tilde{Y}) \right\rangle$$

where the matrix  $\nabla^2 f(Y; \tilde{Y})$  depends linearly on  $\tilde{Y}$ .

The gradient  $\nabla f(X, Y)$  can be found by expanding  $f(X + \epsilon \tilde{X}, Y + \epsilon \tilde{Y})$  around the ordered pair  $(X, Y)$  for the variation  $(\epsilon \tilde{X}, \epsilon \tilde{Y})$  and collecting terms of  $O(\epsilon)$ . This yields,

$$\nabla_X f(X, Y) = Q - X^{-1}Y^*RYX^{-1}, \quad \nabla_Y f(X, Y) = 2RYX^{-1}.$$

To find the Hessian, we expand  $\nabla f(X + \epsilon \tilde{X}, Y + \epsilon \tilde{Y})$ ,

$$\begin{aligned}\nabla_X f(X + \epsilon \tilde{X}, Y) - \nabla_X f(X, Y) &= \epsilon N_1 + O(\epsilon^2) \\ \nabla_X f(X, Y + \epsilon \tilde{Y}) - \nabla_X f(X, Y) &= \epsilon N_2 + O(\epsilon^2) \\ \nabla_Y f(X + \epsilon \tilde{X}, Y) - \nabla_Y f(X, Y) &= \epsilon N_3 + O(\epsilon^2) \\ \nabla_Y f(X, Y + \epsilon \tilde{Y}) - \nabla_Y f(X, Y) &= \epsilon N_4 + O(\epsilon^2)\end{aligned}$$

where the matrices

$$\begin{aligned}N_1 &:= X^{-1}Y^*RYX^{-1}\tilde{X}X^{-1} + X^{-1}\tilde{X}X^{-1}Y^*RYX^{-1} \\ N_2 &:= -X^{-1}\tilde{Y}^*RYX^{-1} - X^{-1}Y^*R\tilde{Y}X^{-1} \\ N_3 &:= -2RYX^{-1}\tilde{X}X^{-1} \\ N_4 &:= 2R\tilde{Y}X^{-1},\end{aligned}$$

depend linearly on  $\tilde{X}$  and  $\tilde{Y}$ . Thus, we arrive at

$$\begin{aligned}\langle (\tilde{X}, \tilde{Y}), \nabla^2 f(X, Y; \tilde{X}, \tilde{Y}) \rangle &= \langle \tilde{X}, N_1(X, Y, \tilde{X}) + N_2(X, Y, \tilde{Y}) \rangle + \langle \tilde{Y}, N_3(X, Y, \tilde{X}) + N_4(X, Y, \tilde{Y}) \rangle \\ &= 2 \|R^{\frac{1}{2}}(\tilde{Y} - YX^{-1}\tilde{X})X^{-\frac{1}{2}}\|_F^2.\end{aligned}$$

The result follows from  $\mathcal{A}_1(\tilde{X}) = \mathcal{B}(\tilde{Y})$ . ■

Let us define  $\zeta: \mathcal{D}_s \times \mathcal{S}_1 \rightarrow \mathbb{R}$  as

$$\zeta(Y, \tilde{Y}) = \langle \tilde{Y}, \nabla^2 f(Y, \tilde{Y}) \rangle$$

where  $\mathcal{S}_1 := \{\tilde{Y} \in \mathbb{C}^{m \times n} \mid \|\tilde{Y}\|_F = 1\}$ . To establish strong convexity of  $f(Y)$  and Lipschitz continuity of its gradient over a compact set  $\mathcal{C}$ , we find a positive lower bound  $\mu$  and an upper bound  $L$  on  $\zeta$ ,  $\mu \leq \zeta(Y, \tilde{Y}) \leq L$ , for all  $(Y, \tilde{Y}) \in \mathcal{C} \times \mathcal{S}_1$ .

Using the expression in Lemma 3, it is straightforward to show that the function  $\zeta$  is continuous. From the continuity of  $\zeta(Y, \tilde{Y})$  and the compactness of  $\mathcal{C} \times \mathcal{S}_1$ , it follows that  $\zeta$  is bounded on  $\mathcal{C} \times \mathcal{S}_1$ . This implies the existence of an upper bound  $L$ . To find a positive lower bound, let  $(Y_o, \tilde{Y}_o)$  be a minimizer of the function  $\zeta(Y, \tilde{Y})$  over the set  $\mathcal{C} \times \mathcal{S}_1$ . The existence of  $(Y_o, \tilde{Y}_o)$  follows from the compactness of  $\mathcal{C} \times \mathcal{S}_1$  and the continuity of the function  $\zeta$ . We next show that  $\mu := \zeta(Y_o, \tilde{Y}_o) > 0$ .

Suppose, for the sake of contradiction, that  $\zeta(Y_o, \tilde{Y}_o) = 0$ . From Lemma 3, we have

$$\tilde{Y}_o = K_o \tilde{X}_o \tag{26}$$

where  $K_o = Y_o X_o^{-1}$ ,  $X_o = X(Y_o)$ , and

$$\tilde{X}_o = \mathcal{M}(\tilde{Y}_o). \tag{27}$$

Combining (27) and the Lyapunov equation in Problem 2 yields

$$\mathcal{A}(X_o + \tilde{X}_o) - \mathcal{B}(Y_o + \tilde{Y}_o) = -V. \quad (28)$$

From (26), we also have

$$Y_o + \tilde{Y}_o = K_o (X_o + \tilde{X}_o). \quad (29)$$

Substituting for  $Y_o + \tilde{Y}_o$  in (28) from (29), we arrive at

$$\mathcal{A}(X_o + \tilde{X}_o) - \mathcal{B}(K_o (X_o + \tilde{X}_o)) = -V.$$

Consequently, both  $X_o$  and  $X_o + \tilde{X}_o$  solve the Lyapunov equation with stabilizing feedback gain  $K_o$ , which is a contradiction. Thus,  $\zeta(Y_o, \tilde{Y}_o)$  is positive. This completes the proof.

2) *Proof of Lemma 1:* We first show that the positive definite matrix  $X = \mathcal{A}_1(\mathcal{B}(Y) - V)$  satisfies

$$\nu I \preceq X, \quad (30)$$

with  $\nu$  given by (18b). Let  $v$  be the normalized eigenvector corresponding to the smallest eigenvalue of  $X$ . Multiplying the Lyapunov equation in Problem 2 from left and right by  $v^*$  and  $v$  gives

$$v^*(DX^{\frac{1}{2}} + X^{\frac{1}{2}}D^*)v = \sqrt{\lambda_{\min}(X)} v^*(D + D^*)v = -v^*Vv,$$

where  $D := AX^{1/2} - B Y X^{-1/2}$ . We thus have

$$\lambda_{\min}(X) = \frac{(v^*Vv)^2}{(v^*(D + D^*)v)^2} \geq \frac{\lambda_{\min}^2(V)}{4\|D\|_2^2}, \quad (31)$$

where we have applied the Cauchy-Schwarz inequality on the denominator. For  $Y \in \mathcal{D}(a)$ , we have

$$\text{trace}(QX + Y^*RYX^{-1}) \leq a.$$

This inequality along with  $\text{trace}(QX) \geq \lambda_{\min}(Q)\|X^{1/2}\|_F^2$  and  $\text{trace}(RYX^{-1}Y^*) \geq \lambda_{\min}(R)\|YX^{-1/2}\|_F^2$  yields

$$\|X^{1/2}\|_F^2 \leq a/\lambda_{\min}(Q), \quad (32a)$$

$$\|YX^{-1/2}\|_F^2 \leq a/\lambda_{\min}(R). \quad (32b)$$

Combination of the triangle inequality, submultiplicative property of the 2-norm, and (32) leads to

$$\|D\|_2 \leq \sqrt{a} \left( \frac{\sigma_{\max}(A)}{\sqrt{\lambda_{\min}(Q)}} + \frac{\sigma_{\max}(B)}{\sqrt{\lambda_{\min}(R)}} \right). \quad (33)$$

Inequality (30), with  $\nu$  given by (18b), follows from combining (31) and (33).

We now show that  $L$  given by (18a) is a Lipschitz continuity parameter of  $\nabla f$ . To do this, we first use (32) to

establish an upper bound on  $\|Y\|_2$ ,

$$\|Y\|_2 \leq \sqrt{\frac{a \lambda_{\max}(X)}{\lambda_{\min}(R)}} \leq \nu',$$

where  $\nu' := a / (\lambda_{\min}(R) \lambda_{\min}(Q))^{1/2}$ . This allows us to upper bound the quadratic form provided in Lemma 3,

$$\langle \tilde{Y}, \nabla^2 f(Y, \tilde{Y}) \rangle = 2 \|R^{\frac{1}{2}}(\tilde{Y} - YX^{-1}\mathcal{M}(\tilde{Y}))X^{-\frac{1}{2}}\|_F^2.$$

In particular, for any  $Y \in \mathcal{D}(a)$  and  $\tilde{Y}$  with  $\|\tilde{Y}\|_F = 1$ , we have

$$\begin{aligned} 2 \|R^{\frac{1}{2}}(\tilde{Y} - YX^{-1}\mathcal{M}(\tilde{Y}))X^{-\frac{1}{2}}\|_F^2 &\leq 2m \|R^{\frac{1}{2}}(\tilde{Y} - YX^{-1}\mathcal{M}(\tilde{Y}))X^{-\frac{1}{2}}\|_2^2 \\ &\leq \frac{2m}{\nu} \lambda_{\max}(R) \left(1 + \frac{\nu' \sigma_{\max}(\mathcal{M})}{\nu}\right)^2 = L, \end{aligned}$$

where the last inequality follows from the sub-multiplicative property and the triangle inequality. This completes the proof.

3) *Proof of Lemma 2:* Without loss of generality, let  $\gamma = 1$ . The existence of the scalar

$$a > \max_{Y \in \mathcal{D}(b)} f(Y) + g(Y)$$

with  $b := f(Y^0) + g(Y^0)$  follows from the compactness of the sublevel set  $\mathcal{D}(b)$  (see the proof of Theorem 1) and the continuity of the function  $f + g$ . Consider the sublevel set

$$\mathcal{E}(b) := \{Y \in \mathcal{D}_s \mid f(Y) + g(Y) \leq b\}.$$

Since  $g$  is nonnegative, we have  $a > b$  and  $\mathcal{E}(b) \subset \mathcal{D}(a)$ .

For a given  $Y \in \mathcal{E}(b)$ , let  $P: \mathbb{R}^+ \rightarrow \mathbb{C}^{m \times n}$  be defined as

$$P(\alpha) = \mathbf{prox}_{\alpha g}(Y - \alpha \nabla f(Y)).$$

Due to the properties of the soft-thresholding operator, the map  $P(\alpha)$  is continuous and  $P(0) = Y$ . In what follows, we show that  $P(\alpha) \in \mathcal{E}(b)$  for all  $\alpha \in [0, 1/L]$ , with  $L$  being the Lipschitz continuity parameter of  $\nabla f(Y)$  over the set  $\mathcal{D}(a)$ . The quadratic function  $l_\alpha: \mathbb{C}^{m \times n} \rightarrow \mathbb{R}$ ,

$$l_\alpha(\hat{Y}) := f(Y) + \langle \nabla f(Y), \hat{Y} - Y \rangle + \frac{1}{2\alpha} \|\hat{Y} - Y\|^2,$$

satisfies

$$f(\hat{Y}) \leq l_\alpha(\hat{Y}) \tag{34}$$

for all  $\hat{Y} \in \mathcal{D}(a)$  and  $\alpha \in [0, 1/L]$  (cf. (17b)). This follows from the  $L$ -Lipschitz continuity of  $\nabla f(Y)$  over  $\mathcal{D}(a)$

(Descent Lemma). Moreover, by definition,

$$P(\alpha) = \underset{\hat{Y} \in \mathbb{C}^{m \times n}}{\operatorname{argmin}} l_\alpha(\hat{Y}) + g(\hat{Y}),$$

and  $l_\alpha(Y) = f(Y)$ , which yields

$$l_\alpha(P(\alpha)) + g(P(\alpha)) \leq f(Y) + g(Y) \leq b \quad (35)$$

for all  $\alpha \geq 0$ . Substituting  $P(\alpha)$  for  $\hat{Y}$  in (34), however, requires showing  $P(\alpha) \in D(a)$  for all  $\alpha \in [0, 1/L]$ .

Let  $\alpha_1$  be the largest scalar such that  $P(\alpha_2) \in \mathcal{D}_s$  and  $f(P(\alpha_2)) \leq a$ , for all  $\alpha_2 \in [0, \alpha_1]$ . It is straightforward to show that the set  $\mathcal{D}_s$  is open. Based on this, and the continuity of functions  $f(Y)$  (on  $\mathcal{D}_s$ ) and  $P(\alpha)$  we conclude that  $\alpha_1 > 0$ . We next show that  $\alpha_1 > 1/L$ . For the sake of contradiction, suppose  $\alpha_1 \leq 1/L$ . From the compactness of  $\mathcal{D}(a)$  and the continuity of  $P(\alpha)$ , it is straightforward to show that

$$P(\alpha_1) \in \mathcal{D}(a).$$

This fact, along with the continuity of  $f(P(\alpha))$ , yields

$$f(P(\alpha_1)) = a.$$

Thus, by substituting  $P(\alpha_1)$  for  $\hat{Y}$  in Eq. (34), we arrive at

$$a = f(P(\alpha_1)) \leq l_\alpha(P(\alpha_1)) \leq b.$$

The last inequality follows from (35), and it contradicts with  $a > b$ . Thus,  $\alpha_1 > 1/L$  which implies that  $P(\alpha) \in \mathcal{D}(a)$  for all  $\alpha \in [0, 1/L]$ . Furthermore, based on this, substituting  $P(\alpha)$  in (34) and utilizing (35) gives

$$f(P(\alpha)) + g(P(\alpha)) \leq b,$$

which in turn implies  $P(\alpha) \in \mathcal{E}(b)$ . This completes the proof.

#### E. Linear convergence with adaptive step-size selection

We provide details on how the backtracking step-size selection satisfying (17) keeps the iterates of the PG algorithm within  $\mathcal{D}(a)$ . As discussed in the proof of Lemma 2, the step-size  $\alpha_k = 1/L$  satisfies conditions (17). Thus, backtracking from a constant initial step-size  $\alpha_{k,0}$  would result in a step-size  $\alpha_k \geq \min\{\alpha_{k,0}, c/L\}$ , where  $c$  is the backtracking parameter in Algorithm 1. The lower bound on  $\alpha_k$  ensures that the PG algorithm maintains its linear rate of convergence, even if combined with backtracking.

On the other hand, the adaptive step-size selection method discussed in Section IV-B1 does not assume  $\alpha_{k,0}$  to be constant. Let  $\Delta_1 := Y^k - Y^{k-1}$  and  $\Delta_2 := \nabla f(Y^k) - \nabla f(Y^{k-1})$ . We show that the step-size initialization

proposed by (16) satisfies  $\alpha_{k,0} \geq 1/(\sqrt{2}L')$ , for any

$$L' \geq \|\Delta_2\|_F / \|\Delta_1\|_F. \quad (36)$$

Assuming  $\langle \Delta_1, \Delta_2 \rangle > 0$ , the steepest descent and minimum residual step-sizes are given by  $\alpha_s = \|\Delta_1\|_F^2 / \langle \Delta_1, \Delta_2 \rangle$  and  $\alpha_m = \langle \Delta_1, \Delta_2 \rangle / \|\Delta_2\|_F^2$ , respectively. If  $\alpha_m / \alpha_s > 1/2$ , then  $\sqrt{2} \langle \Delta_1, \Delta_2 \rangle > \|\Delta_1\| \|\Delta_2\|$ , which yields

$$\alpha_{k,0} = \frac{\langle \Delta_1, \Delta_2 \rangle}{\|\Delta_2\|_F^2} > \frac{\|\Delta_1\|_F}{\sqrt{2}\|\Delta_2\|_F} \geq \frac{1}{\sqrt{2}L'}.$$

On the other hand, if  $\alpha_m / \alpha_s \leq 1/2$ , then  $\sqrt{2} \langle \Delta_1, \Delta_2 \rangle \leq \|\Delta_1\|_F \|\Delta_2\|_F$ , which yields

$$\alpha_{k,0} = \frac{\|\Delta_1\|_F^2}{\langle \Delta_1, \Delta_2 \rangle} - \frac{\langle \Delta_1, \Delta_2 \rangle}{2\|\Delta_2\|_F^2} \geq \frac{3}{2\sqrt{2}} \frac{\|\Delta_1\|_F}{\|\Delta_2\|_F} \geq \frac{3}{2\sqrt{2}L'}.$$

Since  $Y^k, Y^{k-1} \in \mathcal{D}(a)$ , inequality (36) holds with  $L' = L$  the Lipschitz continuity factor of  $\nabla f(Y)$  over  $\mathcal{D}(a)$ . Thus, even in the case of adaptive backtracking, the resulting step-size is lower bounded by  $\alpha_k \geq \min\{1/(\sqrt{2}L), c/L\}$ , guaranteeing a linear convergence rate for the PG algorithm.

#### F. Gradient of $F(Y)$ in (21)

Similar to Appendix C, we expand  $F(Y + \epsilon \tilde{Y})$  around  $Y$  for the variation  $\epsilon \tilde{Y}$ , and collect terms of  $O(\epsilon)$ . Based on this, at the  $k$ th iteration, the gradient of  $F$  with respect to  $Y$  is given by,

$$\nabla F(Y^k) = 2Y^k X^{-1} - 2B^*(W_2 + \rho_k W_3 - W_1),$$

where  $W_1, W_2$ , and  $W_3$  are solutions to the following Lyapunov equations

$$\begin{aligned} A^*W_1 + W_1A + X^{-1}Y^{k*}Y^kX^{-1} &= 0 \\ A^*W_2 + W_2A + \mathcal{A}_2^\dagger(\Lambda^k) &= 0 \\ A^*W_3 + W_3A + \mathcal{A}_2^\dagger(\mathcal{A}_2(X(Y^k)) - G) &= 0 \end{aligned}$$

Here,  $X^{-1}$  denotes the inverse of  $X(Y^k)$  and the adjoint of the operator  $\mathcal{A}_2$  is given by  $\mathcal{A}_2^\dagger(\Lambda) := C^*(E \circ \Lambda)C$ .

#### REFERENCES

- [1] S. Boyd, L. E. Ghaoui, E. Feron, and V. Balakrishnan, *Linear matrix inequalities in system and control theory*. SIAM, 1994.
- [2] G. E. Dullerud and F. Paganini, *A course in robust control theory: a convex approach*. New York: Springer-Verlag, 2000.
- [3] M. Fazel, H. Hindi, and S. Boyd, "A rank minimization heuristic with application to minimum order system approximation," in *Proceedings of the 2001 American Control Conference*, 2001, pp. 4734–4739.
- [4] S. Boyd and L. Vandenberghe, *Convex optimization*. Cambridge University Press, 2004.
- [5] M. Fazel, H. Hindi, and S. Boyd, "Rank minimization and applications in system theory," in *Proceedings of the 2004 American Control Conference*, 2004, pp. 3273–3278.
- [6] Z. Liu and L. Vandenberghe, "Interior-point method for nuclear norm approximation with application to system identification," *SIAM J. Matrix Anal. Appl.*, vol. 31, no. 3, pp. 1235–1256, 2009.
- [7] M. R. Jovanović and N. K. Dhingra, "Controller architectures: tradeoffs between performance and structure," *Eur. J. Control*, vol. 30, pp. 76–91, July 2016.

- [8] A. Zare, Y. Chen, M. R. Jovanović, and T. T. Georgiou, “Low-complexity modeling of partially available second-order statistics: theory and an efficient matrix completion algorithm,” *IEEE Trans. Automat. Control*, vol. 62, no. 3, pp. 1368–1383, March 2017.
- [9] A. Zare, M. R. Jovanović, and T. T. Georgiou, “Colour of turbulence,” *J. Fluid Mech.*, vol. 812, pp. 636–680, February 2017.
- [10] B. F. Farrell and P. J. Ioannou, “Stochastic forcing of the linearized Navier-Stokes equations,” *Phys. Fluids A*, vol. 5, no. 11, pp. 2600–2609, 1993.
- [11] B. Bamieh and M. Dahleh, “Energy amplification in channel flows with stochastic excitation,” *Phys. Fluids*, vol. 13, no. 11, pp. 3258–3269, 2001.
- [12] M. R. Jovanović and B. Bamieh, “Componentwise energy amplification in channel flows,” *J. Fluid Mech.*, vol. 534, pp. 145–183, July 2005.
- [13] R. Moarref and M. R. Jovanović, “Model-based design of transverse wall oscillations for turbulent drag reduction,” *J. Fluid Mech.*, vol. 707, pp. 205–240, September 2012.
- [14] M. R. Jovanović and B. Bamieh, “Modelling flow statistics using the linearized Navier-Stokes equations,” in *Proceedings of the 40th IEEE Conference on Decision and Control*, 2001, pp. 4944–4949.
- [15] A. Zare, M. R. Jovanović, and T. T. Georgiou, “Perturbation of system dynamics and the covariance completion problem,” in *Proceedings of the 55th IEEE Conference on Decision and Control*, 2016, pp. 7036–7041.
- [16] A. Hotz and R. E. Skelton, “Covariance control theory,” *Int. J. Control*, vol. 46, no. 1, pp. 13–32, 1987.
- [17] K. Yasuda, R. E. Skelton, and K. M. Grigoriadis, “Covariance controllers: A new parametrization of the class of all stabilizing controllers,” *Automatica*, vol. 29, no. 3, pp. 785–788, 1993.
- [18] M. K. K. M. Grigoriadis and R. E. Skelton, “Alternating convex projection methods for covariance control design,” *Int. J. Control*, vol. 60, no. 6, pp. 1083–1106, 1994.
- [19] Y. Chen, T. T. Georgiou, and M. Pavon, “Optimal steering of a linear stochastic system to a final probability distribution, Part II,” *IEEE Trans. Automat. Control*, vol. 61, no. 5, pp. 1170–1180, 2016.
- [20] F. Lin and M. R. Jovanović, “Least-squares approximation of structured covariances,” *IEEE Trans. Automat. Control*, vol. 54, no. 7, pp. 1643–1648, July 2009.
- [21] A. Ferrante, M. Pavon, and M. Zorzi, “A maximum entropy enhancement for a family of high-resolution spectral estimators,” *IEEE Trans. Automat. Control*, vol. 57, no. 2, pp. 318–329, 2012.
- [22] M. Zorzi and A. Ferrante, “On the estimation of structured covariance matrices,” *Automatica*, vol. 48, no. 9, pp. 2145–2151, 2012.
- [23] T. H. Summers, F. L. Cortesi, and J. Lygeros, “On submodularity and controllability in complex dynamical networks,” *IEEE Trans. Control Netw. Syst.*, vol. 3, no. 1, pp. 91–101, 2016.
- [24] V. Tzoumas, M. A. Rahimian, G. J. Pappas, and A. Jadbabaie, “Minimal actuator placement with bounds on control effort,” *IEEE Trans. Control Netw. Syst.*, vol. 3, no. 1, pp. 67–78, 2016.
- [25] H. Zhang, R. Ayoub, and S. Sundaram, “Sensor selection for kalman filtering of linear dynamical systems: Complexity, limitations and greedy algorithms,” *Automatica*, vol. 78, pp. 202–210, 2017.
- [26] A. Olshevsky, “On (non)supermodularity of average control energy,” *IEEE Trans. Control Netw. Syst.*, vol. 5, no. 3, pp. 1177–1181, 2018.
- [27] S. Joshi and S. Boyd, “Sensor selection via convex optimization,” *IEEE Trans. Signal Process.*, vol. 57, no. 2, pp. 451–462, 2009.
- [28] S. Liu, S. P. Chepuri, M. Fardad, E. Maşazade, G. Leus, and P. K. Varshney, “Sensor selection for estimation with correlated measurement noise,” *IEEE Trans. Signal Process.*, vol. 64, no. 13, pp. 3509–3522, 2016.
- [29] V. Kekatos, G. B. Giannakis, and B. Wollenberg, “Optimal placement of phasor measurement units via convex relaxation,” *IEEE Trans. Power Syst.*, vol. 27, no. 3, pp. 1521–1530, 2012.
- [30] J. L. Rogers, “A parallel approach to optimum actuator selection with a genetic algorithm,” in *AIAA Guidance, Navigation, and Control Conference*, 2000, pp. 14–17.
- [31] S. Kondoh, C. Yatomi, and K. Inoue, “The positioning of sensors and actuators in the vibration control of flexible systems,” *JSME Int. J., Ser. III*, vol. 33, no. 2, pp. 145–152, 1990.
- [32] K. Hiramoto, H. Doki, and G. Obinata, “Optimal sensor/actuator placement for active vibration control using explicit solution of algebraic Riccati equation,” *J. Sound Vib.*, vol. 229, no. 5, pp. 1057–1075, 2000.
- [33] K. K. Chen and C. W. Rowley, “ $\mathcal{H}_2$  optimal actuator and sensor placement in the linearised complex Ginzburg-Landau system,” *J. Fluid Mech.*, vol. 681, pp. 241–260, 2011.

- [34] M. Fardad, F. Lin, and M. R. Jovanović, “Sparsity-promoting optimal control for a class of distributed systems,” in *Proceedings of the 2011 American Control Conference*, 2011, pp. 2050–2055.
- [35] F. Lin, M. Fardad, and M. R. Jovanović, “Sparse feedback synthesis via the alternating direction method of multipliers,” in *Proceedings of the 2012 American Control Conference*, 2012, pp. 4765–4770.
- [36] F. Lin, M. Fardad, and M. R. Jovanović, “Design of optimal sparse feedback gains via the alternating direction method of multipliers,” *IEEE Trans. Automat. Control*, vol. 58, no. 9, pp. 2426–2431, September 2013.
- [37] E. Masazade, M. Fardad, and P. K. Varshney, “Sparsity-promoting extended Kalman filtering for target tracking in wireless sensor networks,” *IEEE Signal Process. Lett.*, vol. 19, pp. 845–848, 2012.
- [38] S. Liu, M. Fardad, E. Masazade, and P. K. Varshney, “Optimal periodic sensor scheduling in networks of dynamical systems,” *IEEE Trans. Signal Process.*, vol. 62, no. 12, pp. 3055–3068, 2014.
- [39] B. Polyak, M. Khlebnikov, and P. Shcherbakov, “An LMI approach to structured sparse feedback design in linear control systems,” in *Proceedings of the 2013 European Control Conference*, 2013, pp. 833–838.
- [40] U. Münz, M. Pfister, and P. Wolfrum, “Sensor and actuator placement for linear systems based on  $\mathcal{H}_2$  and  $\mathcal{H}_\infty$  optimization,” *IEEE Trans. Automat. Control*, vol. 59, no. 11, pp. 2984–2989, 2014.
- [41] M. Yuan and Y. Lin, “Model selection and estimation in regression with grouped variables,” *J. R. Stat. Soc. Series B Stat. Methodol.*, vol. 68, no. 1, pp. 49–67, 2006.
- [42] R. A. Horn and C. R. Johnson, *Matrix Analysis*. Cambridge University Press, 2012.
- [43] A. Beck and M. Teboulle, “A fast iterative shrinkage-thresholding algorithm for linear inverse problems,” *SIAM J. Imaging Sci.*, vol. 2, no. 1, pp. 183–202, 2009.
- [44] N. Parikh and S. Boyd, “Proximal algorithms,” *Found. Trends Optim.*, vol. 1, no. 3, pp. 123–231, 2013.
- [45] T. Goldstein, C. Studer, and R. Baraniuk, “A field guide to forward-backward splitting with a FASTA implementation,” arXiv:1411.3406, 2014.
- [46] B. Zhou, L. Gao, and Y.-H. Dai, “Gradient methods with adaptive step-sizes,” *Comput. Optim. Appl.*, vol. 35, no. 1, pp. 69–86, 2006.
- [47] A. Beck, *First-Order Methods in Optimization*. SIAM, 2017, vol. 25.
- [48] D. P. Bertsekas, *Constrained optimization and Lagrange multiplier methods*. New York: Academic Press, 1982.
- [49] D. P. Bertsekas, *Nonlinear programming*. Belmont, MA: Athena Scientific, 1999.
- [50] J. Nocedal and S. J. Wright, *Numerical Optimization*. Springer, 2006.
- [51] S. Boyd, N. Parikh, E. Chu, B. Peleato, and J. Eckstein, “Distributed optimization and statistical learning via the alternating direction method of multipliers,” *Found. Trends Mach. Learn.*, vol. 3, no. 1, pp. 1–122, 2011.
- [52] N. K. Dhingra, M. R. Jovanović, and Z. Q. Luo, “An ADMM algorithm for optimal sensor and actuator selection,” in *Proceedings of the 53rd IEEE Conference on Decision and Control*, 2014, pp. 4039–4044.
- [53] E. J. Candes, M. B. Wakin, and S. P. Boyd, “Enhancing sparsity by reweighted  $\ell_1$  minimization,” *J. Fourier Anal. Appl.*, vol. 14, no. 5-6, pp. 877–905, 2008.
- [54] M. C. Cross and P. C. Hohenberg, “Pattern formation outside of equilibrium,” *Rev. Mod. Phys.*, vol. 65, no. 3, p. 851, 1993.
- [55] J. Burke and E. Knobloch, “Localized states in the generalized Swift-Hohenberg equation,” *Phys. Rev. E*, vol. 73, no. 5, p. 056211, 2006.
- [56] K.-C. Toh, M. J. Todd, and R. H. Tütüncü, “SDPT3-a MATLAB software package for semidefinite programming, version 1.3,” *Optim. Methods Softw.*, vol. 11, no. 1-4, pp. 545–581, 1999.
- [57] M. Grant and S. Boyd, “CVX: Matlab software for disciplined convex programming, version 2.1,” <http://cvxr.com/cvx>, Mar. 2014.
- [58] T. Summers, “Actuator placement in networks using optimal control performance metrics,” in *Proceedings of the 55th IEEE Conference on Decision and Control*, 2016, pp. 2703–2708.
- [59] C. Grussler, A. Zare, M. R. Jovanović, and A. Rantzer, “The use of the  $r^*$  heuristic in covariance completion problems,” in *Proceedings of the 55th IEEE Conference on Decision and Control*, 2016, pp. 1978–1983.
- [60] C. Grussler, “Rank reduction with convex constraints,” Ph.D. dissertation, Lund University, 2017.
- [61] N. K. Dhingra, S. Z. Khong, and M. R. Jovanović, “A second order primal-dual method for nonsmooth convex composite optimization,” *IEEE Trans. Automat. Control*, 2017, submitted; also arXiv:1709.01610.
- [62] N. K. Dhingra, S. Z. Khong, and M. R. Jovanović, “The proximal augmented Lagrangian method for nonsmooth composite optimization,” *IEEE Trans. Automat. Control*, 2018, doi:10.1109/TAC.2018.2867589.



- [63] J. D. Lee, Y. Sun, and M. A. Saunders, “Proximal Newton-type methods for minimizing composite functions,” *SIAM J. Optim.*, vol. 24, no. 3, pp. 1420–1443, 2014.
- [64] L. Stella, A. Themelis, and P. Patrinos, “Forward-backward quasi-Newton methods for nonsmooth optimization problems,” *Comput. Optim. Appl.*, vol. 67, no. 3, pp. 443–487, 2017.
- [65] H. T. Toivonen, “A globally convergent algorithm for the optimal constant output feedback problem,” *Int. J. Control*, vol. 41, no. 6, pp. 1589–1599, 1985.